OAK RIDGE
NATIONAL LABORATORY
MANAGED BY UT-BATTELLE
FOR THE DEPARTMENT OF ENERGY

ORNL/TM-2006/136

Design Study for a Low-Enriched Uranium Core for the High Flux Isotope Reactor, Annual Report for FY 2006

November 2006

Prepared by
R. T. Primm III
R. J. Ellis
J. C. Gehin
K. T. Clarno
K. A. Williams
D. L. Moses

UT-BATTELLE
ORNL-27 (4-00)

ORNL/TM-2006/136

DESIGN STUDY FOR A LOW-ENRICHED URANIUM CORE FOR THE HIGH FLUX ISOTOPE REACTOR, ANNUAL REPORT FOR FY 2006

R. T. Primm III
R. J. Ellis
J. C. Gehin
K. T. Clarno
K. A. Williams
D. L. Moses

Date Published: November 2006

Prepared by
OAK RIDGE NATIONAL LABORATORY
Oak Ridge, Tennessee 37831-6283
managed by
UT-BATTELLE, LLC
for the
U.S. DEPARTMENT OF ENERGY
under contract DE-AC05-00OR22725

CONTENTS

Page

LIST OF FIGURES

LIST OF TABLES

ACKNOWLEDGEMENTS

The authors would like to acknowledge that the support for this project was provided by the Reduced Enrichment for Research and Test Reactors Program, Nuclear National Security Administration, U.S. Department of Energy (DOE). The DOE program manager, Parrish Staples, Idaho National Laboratory RERTR fuels program manager, Mitch Meyer, and Argonne National Laboratory RERTR reactor analysis program manager, Jim Matos, all provided useful comments and reviews of this work. The authors also acknowledge the technical reviews of this document preformed by K. A. Smith, Research Reactors Division, and Brian D. Murphy, Nuclear Science and Technology Division, Oak Ridge National Laboratory and thank all of the reviewers for their efforts and comments. Michael I. Morris generated the schedule shown in Section 4 of this report. Finally, the authors wish to thank Cynthia Southmayd and Brenda Smith for their excellence in document preparation and editing of this report.

ABSTRACT

Neutronics and thermal-hydraulics studies show that, for equivalent operating power [85 MW(t)], a low-enriched uranium (LEU) fuel cycle based on uranium-10 wt % molybdenum (U-10Mo) metal foil with radially, “continuously graded” fuel meat thickness results in a 15% reduction in peak thermal flux in the beryllium reflector of the High Flux Isotope Reactor (HFIR) as compared to the current highly enriched uranium (HEU) cycle. The uranium-235 content of the LEU core is almost twice the amount of the HEU core when the length of the fuel cycle is kept the same for both fuels. Because the uranium-238 content of an LEU core is a factor of 4 greater than the uranium-235 content, the LEU HFIR core would weigh 30% more than the HEU core.

A minimum U-10Mo foil thickness of 84 μm is required to compensate for power peaking in the LEU core although this value could be increased significantly without much penalty. The maximum U-10Mo foil thickness is 457μm. Annual plutonium production from fueling the HFIR with LEU is predicted to be 2 kg. For dispersion fuels, the operating power for HFIR would be reduced considerably below 85 MW due to thermal considerations and due to the requirement of a 26-d fuel cycle.

If an acceptable fuel can be developed, it is estimated that $140 M would be required to implement the conversion of the HFIR site at Oak Ridge National Laboratory from an HEU fuel cycle to an LEU fuel cycle. To complete the conversion by fiscal year 2014 would require that all fuel development and qualification be completed by the end of fiscal year 2009. Technological development areas that could increase the operating power of HFIR are identified as areas for study in the future.

1. INTRODUCTION

Design studies for a low-enriched uranium (LEU) core for the High Flux Isotope Reactor (HFIR) were conducted according to the plan documented in Ref. 1. A list of the studies conducted during fiscal year 2006 is presented in Table 1.1 (from Ref. 1). The results of these studies are presented in this document. While these results are considered preliminary, the computer programs and data libraries are the certified versions used in routine safety analysis studies at HFIR and are the versions that are the computational basis for recent updates to the reactor physics and thermal-hydraulics sections of the Safety Analysis Report for HFIR. Likewise, the reactor models that are the starting point for the LEU design studies are the certified versions used for safety analyses of HFIR (Refs. 2–6). These methods and models are described in Ref. 1 with some additional comments provided in Appendix A.

Neutronics and thermal-hydraulics studies performed during fiscal year 2006 were for five variations of U-10Mo fuel. Four of these cases are described in Ref. 1. An additional case added to the study following the publication of Ref. 1 was to remove any minimum thickness constraint on the U-10Mo foil. A preliminary report was published as Ref. 7. Information and conclusions presented in this document supersede Ref. 7.

The results of the reactor core design study were taken as input to an economic and engineering assessment of the modifications required to the HFIR site to accomplish a conversion to LEU fuel if an acceptable fuel can be developed. The assessment is cursory yet provides an "order-of-magnitude" assessment of the costs and calendar time required to accomplish the conversion.

Table 1.1. Quantities to be computed in HFIR LEU study

Safety parameters

- Doppler reactivity coefficient
- Void reactivity coefficient
- Control element differential reactivity worth
- Safety rod reactivity worth (with one stuck element)
- Central void maximum reactivity worth
- Fuel element criticality (elements together and separate in light water and reflected by concrete)
- Fuel element decay heat

Performance parameters

- Cycle length
- Power distribution
- Neutron flux in the central target region
- Peak unperturbed thermal flux in the reflector
- Thermal neutron flux at the HB-2 beam tube
- Thermal neutron flux at the NAA irradiation locations
- Cold source neutron flux

Other parameters (safeguards and environmental)

- Plutonium content in spent fuel elements
- Fuel element dose rates
- Fuel element isotopic compositions

2. MONOLITHIC FUELS

Monolithic fuels, monolith meaning cast as a single piece, that are considered in these studies contain 19.75 wt % ^{235}U in uranium intimately mixed with natural molybdenum such that 10 wt % of the alloy is molybdenum. The monoliths are thin (a few hundred micrometers) and are commonly designated as "foils." For HFIR, the monoliths would have a width of approximately 7.5 cm (about 3 in.) and a length of 50.8 cm (20 in.). The maximum thickness of a foil would be 762 μm (30 mils). However the thickness will vary across the 7.5-cm dimension of the plate (termed the radial direction of the plate). At any given distance along the plate, the thickness of the foil will be constant in the axial direction, that is, the 51-cm-long direction of the plate.

2.1 CONSTRAINED MINIMUM THICKNESS

This case is described in Sect. 3.2.1.1 of Ref. 1. The minimum thickness of the fuel zone inside the plate was constrained to be no less than 127 μm (5 mils). Preliminary results were provided in Ref. 7. However errors in matching the geometric mesh in the neutronics calculation to the mesh in the thermal-hydraulics calculation coupled with differing definitions of the energy cutoff for fast flux as defined by some of the authors of that report led to some inaccuracies in the reporting of performance parameters; performance parameters being defined in Table 1.1. The calculations and definitions were corrected, and physics and thermal parameters were reported in Refs. 8 and 9. Results from those calculations are reported again here for ease of comparison with subsequent cases.

Table 2.1 contains the calculated foil thickness profile that provides for the maximum operating power for the reactor while meeting core lifetime requirements. The table also provides the values for the current HEU fuel. The quantity of ^{235}U in the LEU core is 17.92 kg (90 kg total U). The current, HEU core contains 9.4 kg ^{235}U (10.1 kg total U).

The peak thermal flux in the reflector was 1.73 (10^{13}) neutrons/(cm^2 * s * MW). The value for the current HEU cycle is 2.06 (10^{13}) neutrons/(cm^2 * s * MW). The operating power determined by thermal-hydraulic limits for the reactor was determined to be 84.42 MW. This operating power is considerably greater than the value reported in Ref. 7 due to using Monte Carlo derived power profiles rather than diffusion theory [which was the basis for the calculations in Ref. 7, see Appendix A (Refs. 10–14) for additional comments].

2.2 UNCONSTRAINED MINIMUM THICKNESS

Following the publication of Ref. 7, the Reduced Enrichment for Research and Test Reactor (RERTR) program requested that Oak Ridge National Laboratory (ORNL) staff investigate the case in

Table 2.1. Comparison of fuel meat thicknesses for HEU and constrained minimum thickness LEU fuel plates

Distance along inner element plate (cm)	Thickness of fuel meat				Distance along outer element plate (cm)	Thickness of fuel meat			
	LEU		HEU			LEU		HEU	
	(μm)	(mils)	(μm)	(mils)		(μm)	(mils)	(μm)	(mils)
0.252	127	5	259	10.2	0.191	229	9.0	389	15.3
0.448	127	5.0	295	11.6	0.216	251	9.9	396	15.6
1.203	188	7.4	394	15.5	0.395	356	14.0	429	16.9
2.439	257	10.1	521	20.5	1.134	457	18.0	584	23.0
3.811	300	11.8	620	24.4	2.256	457	18.0	688	27.1
5.314	310	12.2	625	24.6	3.449	401	15.8	648	25.5
6.969	277	10.9	546	21.5	4.655	259	10.2	526	20.7
7.985	213	8.4	472	18.6	5.908	170	6.7	373	14.7
8.091	208	8.2	465	18.3	6.731	135	5.3	292	11.5

which there was no minimum constraint on the thickness of the foil. At that time, this parameter appeared to be the cause of the local power density value that constrained the operating power of the reactor.

The fuel profile that provides the highest operating power is shown in Table 2.2. The peak thermal flux in the reflector was 1.72 (10^{13}) neutron/(cm^2 * s * MW). The value for the current HEU cycle is 2.06 (10^{13}) neutron/(cm^2 * s * MW). The quantity of ^{235}U in the core was 17.54 kg.

The data shown in Table 2.2 are displayed in Figs. 2.1 and 2.2 along with the profiles for the current HEU fuel. The higher ^{235}U density for LEU, relative to HEU, results in considerably thinner fuel meat thicknesses for the LEU plates.

Table 2.2. Comparison of fuel meat thicknesses for LEU (unconstrained minimum thickness) and HEU fuel plates

Distance along inner element plate (cm)	Thickness of fuel meat				Distance along outer element plate (cm)	Thickness of fuel meat			
	LEU		HEU			LEU		HEU	
	(μm)	(mils)	(μm)	(mils)		(μm)	(mils)	(μm)	(mils)
0.252	84	3.3	259	10.2	0.191	152	6.0	389	15.3
0.448	91	3.6	295	11.6	0.216	170	6.7	396	15.6
1.203	99	3.9	394	15.5	0.395	262	10.3	429	16.9
2.439	165	6.5	521	20.5	1.134	378	14.9	584	23.0
3.811	213	8.4	620	24.4	2.256	455	17.9	688	27.1
5.314	224	8.8	625	24.6	3.449	437	17.2	648	25.5
6.969	185	7.3	546	21.5	4.655	320	12.6	526	20.7
7.985	140	5.5	472	18.6	5.908	203	8.0	373	14.7
8.091	137	5.4	465	18.3	6.731	170	6.7	292	11.5

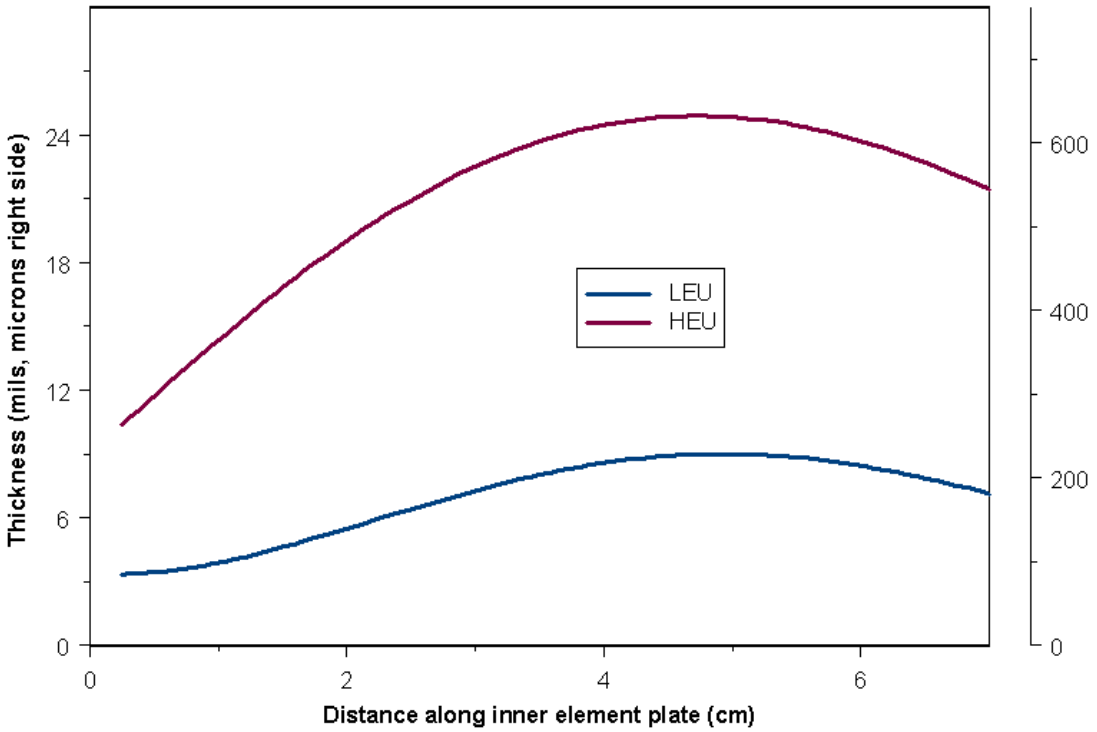

Fig. 2.1. HFIR inner element fuel profile.

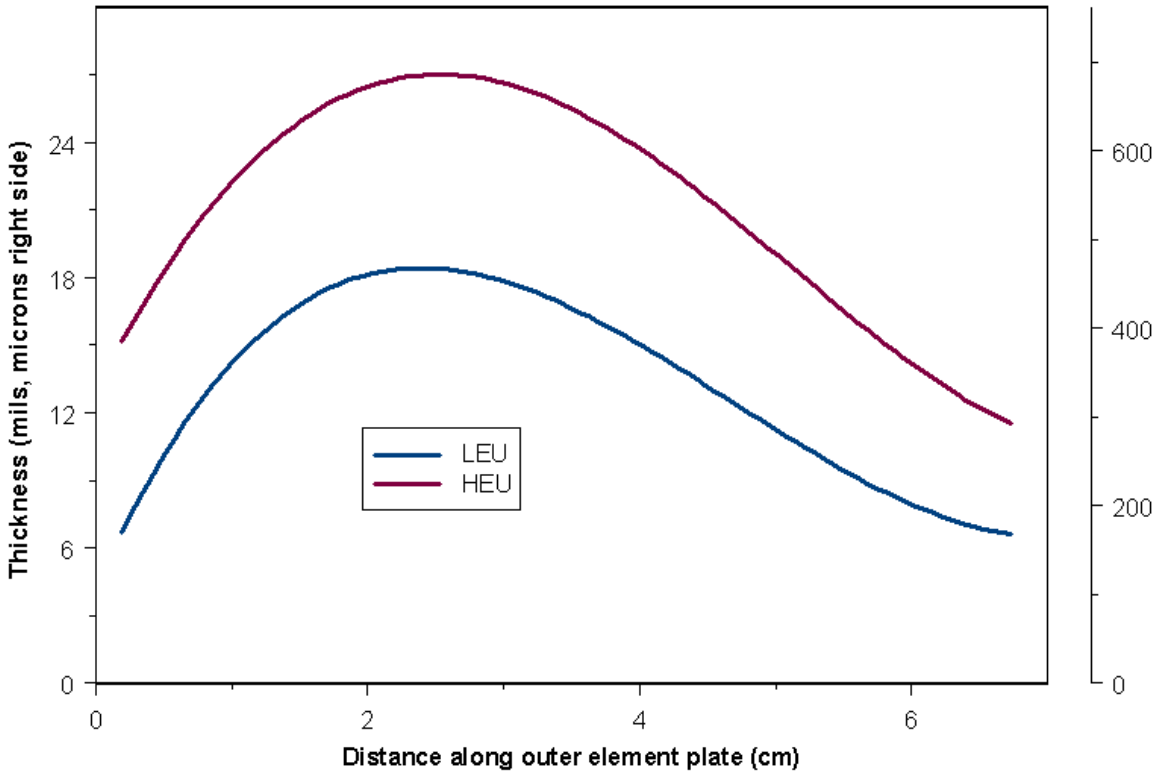

Fig. 2.2. HFIR outer element fuel profile.

The operating power for the reactor was determined to be 84.96 MW. The gain in power level by removing the constraint on minimum thickness was insignificant. This finding, though unexpected, was due to Ref. 7 results (and the program direction based on those results) being based on diffusion theory and to the physics discussion contained in Appendix A. A preliminary assessment by the HFIR fuel fabricator indicated that the cost of fabricating fuel with a minimum thickness of 84 μm (3.3 mils) would be significantly greater than fabricating a foil with a minimum thickness of 127 μm (5 mils).

2.2.1 Performance Parameters

Performance parameters corresponding to entries in Table 1.1 are reported in Table 2.3. This information is repeated in Table 2.4 with the thermal neutron flux level normalized by the reactor power level (85 MW). Both beginning-of-life (BOL) and end-of-life (EOL) values are reported. HB2 refers to the location of the tip of the HB2 beam tube. ISVXF-7 and EF3 refer to the two neutron activation positions in the beryllium reflector.

Table 2.3. Performance parameters (85 MW, unperturbed thermal flux, in neutron/cm^2/s)

Parameter	LEU		HEU		% Difference	
	BOL	EOL	BOL	EOL	BOL	EOL
Central target	$2.522 \times 10^{+15}$	$2.489 \times 10^{+15}$	$2.647 \times 10^{+15}$	$2.704 \times 10^{+15}$	–4.72	–7.95
Peak in beryllium (cold neutron source)	$1.105 \times 10^{+15}$	$1.462 \times 10^{+15}$	$1.145 \times 10^{+15}$	$1.728 \times 10^{+15}$	–3.49	–15.39
HB2	$9.625 \times 10^{+14}$	$1.267 \times 10^{+15}$	$1.001 \times 10^{+15}$	$1.433 \times 10^{+15}$	–3.85	–11.58
ISVXF-7	$8.086 \times 10^{+14}$	$1.061 \times 10^{+15}$	$8.442 \times 10^{+14}$	$1.190 \times 10^{+15}$	–4.22	–10.84
EF3	$3.192 \times 10^{+14}$	$4.100 \times 10^{+14}$	$3.359 \times 10^{+14}$	$4.560 \times 10^{+14}$	–4.97	–10.09

Table 2.4. Normalized performance parameters (flux/power normalizations; neutron/cm^2/s/MW)

Parameter	LEU		HEU	
	BOL	EOL	BOL	EOL
Central target	$2.967 \times 10^{+7}$	$2.929 \times 10^{+7}$	$3.114 \times 10^{+7}$	$3.182 \times 10^{+7}$
Peak in beryllium (cold neutron source)	$1.300 \times 10^{+7}$	$1.720 \times 10^{+7}$	$1.347 \times 10^{+7}$	$2.033 \times 10^{+7}$
HB2	$1.132 \times 10^{+7}$	$1.491 \times 10^{+7}$	$1.178 \times 10^{+7}$	$1.686 \times 10^{+7}$
ISVXF-7	$9.513 \times 10^{+6}$	$1.248 \times 10^{+7}$	$9.932 \times 10^{+6}$	$1.400 \times 10^{+7}$
EF3	$3.755 \times 10^{+6}$	$4.824 \times 10^{+6}$	$3.952 \times 10^{+6}$	$5.365 \times 10^{+6}$

The fuel cycle length for this case is 26 d at a power level of 85 MW [methodology and computational studies provided in Appendix B (Ref. 15)]. The exact value has some uncertainty because the "bias" in the end-of-life k-effective as calculated for the current HEU cycle will not necessarily be the same value that should be used to adjust the calculation for the LEU fuel cycle. The effect is expected to be small and is ignored for the results reported here.

The power distributions at BOL for the inner and outer elements are shown in Figs. 2.3 and 2.4, respectively. These values are from MCNP calculations and have an uncertainty of 1–3%. Radial neutron flux profiles at HFIR midplane for the current HEU fueled core and the unconstrained LEU minimum fuel thickness are shown in Figs. 2.5 and 2.6. The boundaries corresponding to the four energy groups noted in Figs. 2.5 and 2.6 are 20 MeV, 0.085 MeV, 90 eV, 0.625 eV, and $1.0(10^{-5})$ eV. The important thermal neutron flux (the 4th group in Figs. 2.5 and 2.6) is defined as less than 0.625 eV.

The cold neutron source location is the most significant of the performance parameters. The reduction in performance, about 15%, is greatest in this location.

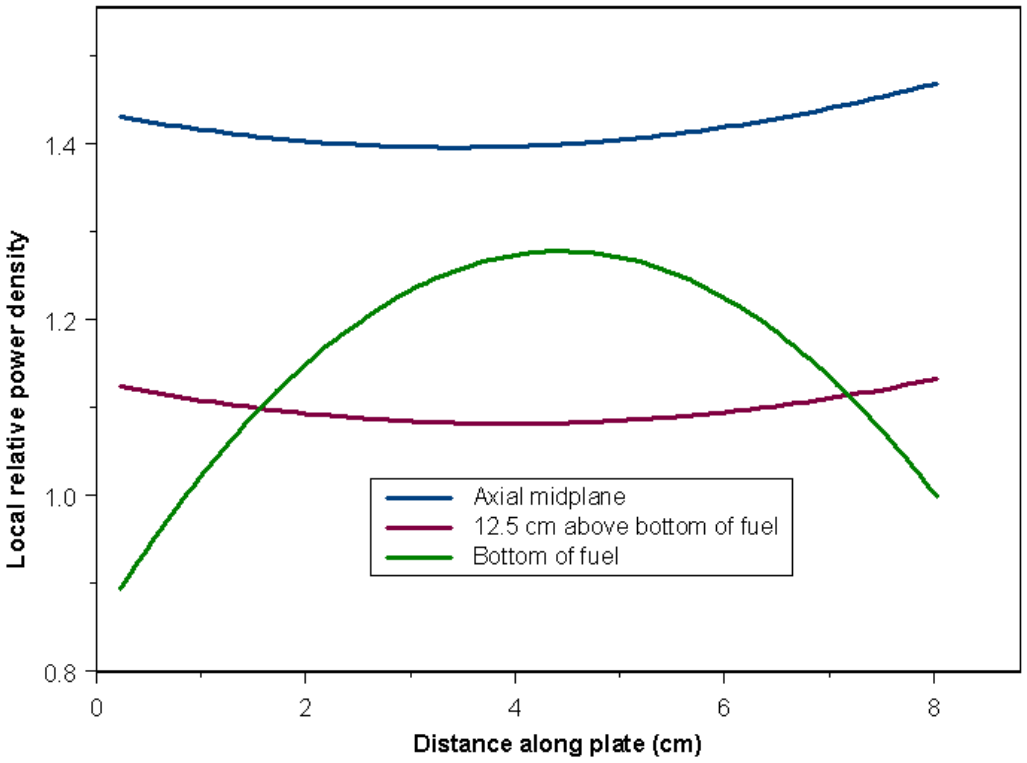

Fig. 2.3. BOL power distribution in inner element of LEU unconstrained minimum thickness core.

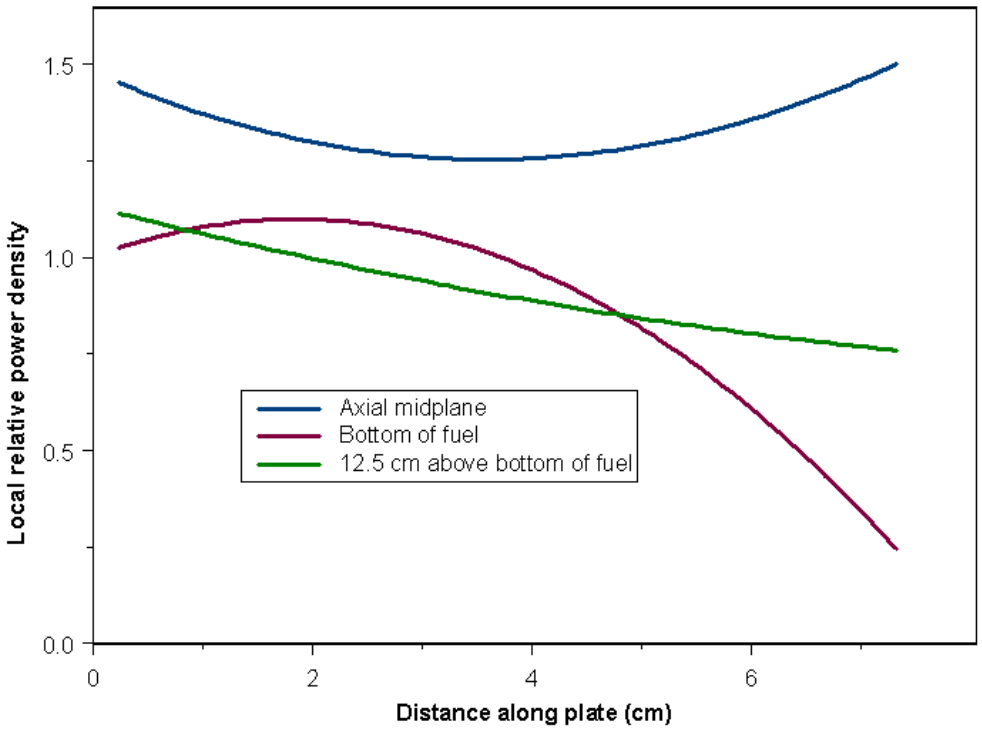

Fig. 2.4. BOL power distribution in outer element of LEU unconstrained minimum thickness core.

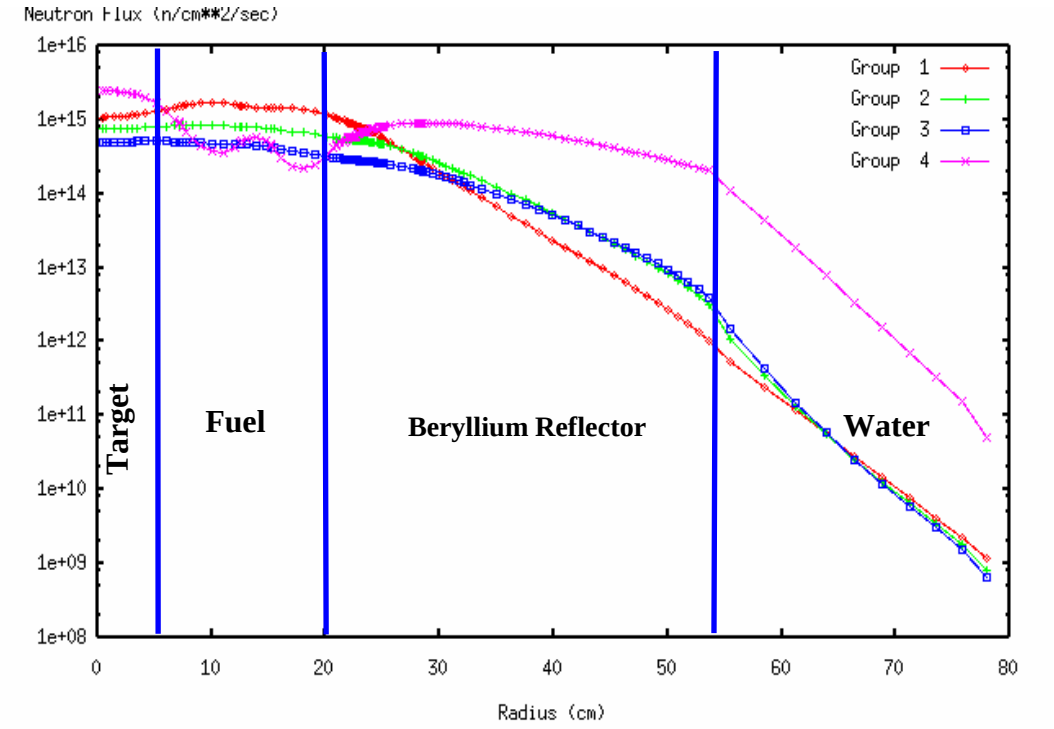

Fig. 2.5. HEU case with control absorber insertion, core midplane at BOL.

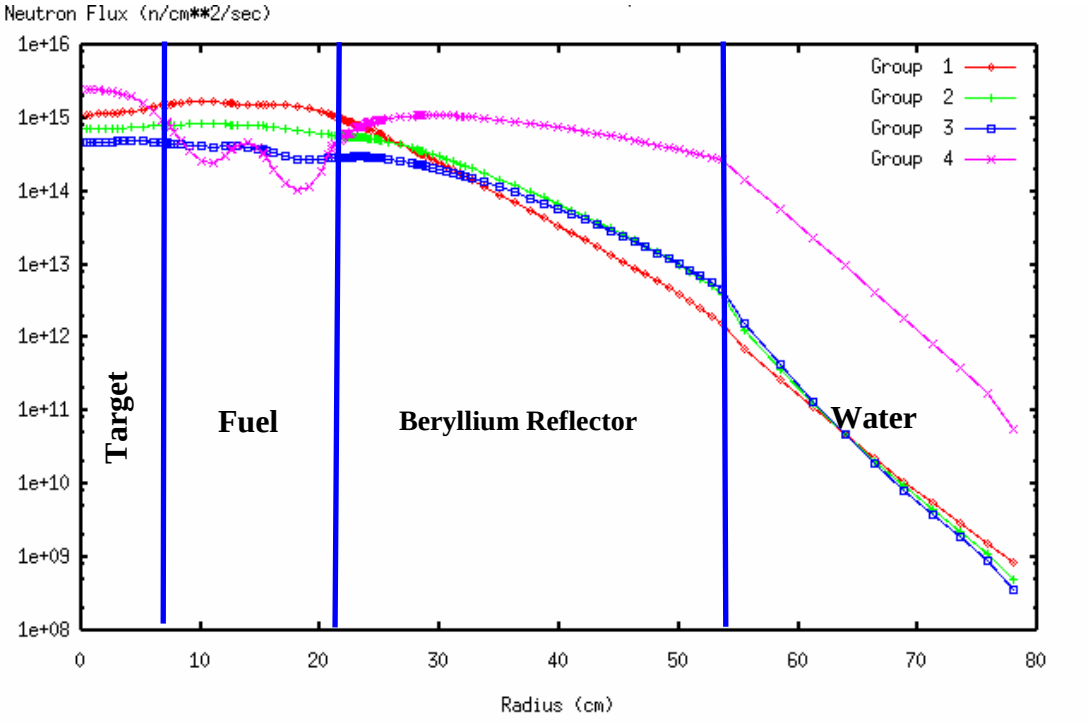

Fig. 2.6. LEU case, with control insertion, core midplane at BOL.

2.2.2 Safety Parameters

Safety-related reactivity coefficients needed for transient analyses are presented in Table 2.5. The methodology for calculating these coefficients is described in Appendix C. It is evident that the Doppler effect is about ten times larger for the LEU case than the HEU case, which is expected in consideration of the large concentration of ^{238}U in the LEU case. The LEU and HEU cores have similar core void reactivity coefficients. The void effect for the central target region is seen to be positive for both the LEU and HEU cases, as expected, and the magnitude of the LEU case values is slightly smaller than the HEU case values. The maximum central void reactivity worth for the LEU core, i.e. searching for the optimal void fraction, was not calculated but can be expected to be less than that of the HEU core due to the reduction in neutron leakage from the LEU core relative to the HEU core.

Table 2.5. Safety coefficients of reactivity

Reactivity coefficient	LEU		HEU	
	BOL	EOL	BOL	EOL
Doppler (300K to 500K)	-2.42×10^{-5} %ΔK/K/C	-2.38×10^{-5} %ΔK/K/C	-2.41×10^{-6} %ΔK/K/C	-2.46×10^{-6} %ΔK/K/C
Void (10%)				
Outer element	–0.0793 %ΔK/K/%v	–0.0679 %ΔK/K/%v	–0.0765 %ΔK/K/%v	–0.0558 %ΔK/K/%v
Inner element	–0.156 %ΔK/K/%v	–0.136 %ΔK/K/%v	–0.185 %ΔK/K/%v	–0.135 %ΔK/K/%v
Central target region	+0.0211 %ΔK/K/%v	+0.0266 %ΔK/K/%v	+0.0265 %ΔK/K/%v	+0.0317 %ΔK/K/%v

A comparison of decay heat generation is provided in Table 2.6. The expected decay heat generation from the two cores is very similar, with the HEU core generating slightly more after heat in the time period from 0.5 year to 5 years. At times approaching 30 years, the actinide contribution to decay heat dominates and the LEU fuel decay heat is slightly greater than HEU though the difference between total decay heats is within the uncertainty of the calculations. The decay heat for the LEU case at the time of discharge from the reactor is greater than that of the HEU core by virtue of the greater production of trans-uranium actinides in LEU (due to the greater ^{238}U content in LEU relative to HEU) and the differing fission product distribution between the two fuels as presented in Tables 2.7 and 2.8.

Table 2.6. Safety parameters: decay heat (W) for the HFIR HEU and LEU cores

Decay heat		Discharge	0.5 year	1 year	5 years	30 years
HEU	Actinides	$4.099 \times 10^{+3}$	3.874×10^{-1}	3.861×10^{-1}	3.823×10^{-1}	3.472×10^{-1}
	FP	$4.409 \times 10^{+6}$	$4.611 \times 10^{+3}$	$1.409 \times 10^{+3}$	$1.123 \times 10^{+2}$	$4.182 \times 10^{+1}$
	Total	$4.413 \times 10^{+6}$	$4.611 \times 10^{+3}$	$1.409 \times 10^{+3}$	$1.127 \times 10^{+2}$	$4.217 \times 10^{+1}$
LEU	Actinides	$7.854 \times 10^{+4}$	$1.233 \times 10^{+0}$	$1.234 \times 10^{+0}$	$1.245 \times 10^{+0}$	$1.262 \times 10^{+0}$
	FP	$5.024 \times 10^{+6}$	$4.583 \times 10^{+3}$	$1.401 \times 10^{+3}$	$1.094 \times 10^{+2}$	$4.124 \times 10^{+1}$
	Total	$5.103 \times 10^{+6}$	$4.584 \times 10^{+3}$	$1.402 \times 10^{+3}$	$1.106 \times 10^{+2}$	$4.250 \times 10^{+1}$

Table 2.7. The top 21 fission product nuclides contributing to decay heat at discharge

LEU		HEU	
Fission product nuclide	**Decay heat contribution (W)**	**Fission product nuclide**	**Decay heat contribution (W)**
^{134}I	$1.02 \times 10^{+5}$	^{134}I	$8.91 \times 10^{+4}$
^{138}Cs	$9.69 \times 10^{+4}$	^{138}Cs	$8.53 \times 10^{+4}$
^{140}Cs	$9.06 \times 10^{+4}$	^{140}Cs	$8.00 \times 10^{+4}$
^{91}Rb	$8.53 \times 10^{+4}$	^{91}Rb	$7.67 \times 10^{+4}$
^{95}Sr	$7.99 \times 10^{+4}$	^{95}Sr	$7.10 \times 10^{+4}$
^{144}La	$7.95 \times 10^{+4}$	^{144}La	$7.06 \times 10^{+4}$
^{92}Rb	$7.66 \times 10^{+4}$	^{92}Rb	$6.85 \times 10^{+4}$
^{100}Nb	$7.63 \times 10^{+4}$	^{93}Sr	$6.78 \times 10^{+4}$
^{93}Sr	$7.62 \times 10^{+4}$	^{142}La	$6.65 \times 10^{+4}$
^{142}La	$7.53 \times 10^{+4}$	^{100}Nb	$6.65 \times 10^{+4}$
^{90}Rb	$7.18 \times 10^{+4}$	^{90}Rb	$6.49 \times 10^{+4}$
^{96}Y	$7.05 \times 10^{+4}$	^{96}Y	$6.21 \times 10^{+4}$
^{95}Y	$6.68 \times 10^{+4}$	^{95}Y	$5.92 \times 10^{+4}$
^{94}Y	$6.60 \times 10^{+4}$	^{94}Y	$5.87 \times 10^{+4}$
^{98}Nb	$6.11 \times 10^{+4}$	^{140}La	$5.41 \times 10^{+4}$
^{99}Zr	$5.89 \times 10^{+4}$	^{98}Nb	$5.34 \times 10^{+4}$
^{93}Rb	$5.72 \times 10^{+4}$	^{99}Zr	$5.15 \times 10^{+4}$
^{89}Rb	$5.67 \times 10^{+4}$	^{89}Rb	$5.11 \times 10^{+4}$
^{89}Kr	$5.59 \times 10^{+4}$	^{93}Rb	$5.08 \times 10^{+4}$
^{94}Sr	$5.43 \times 10^{+4}$	^{89}Kr	$5.05 \times 10^{+4}$
^{140}La	$5.42 \times 10^{+4}$	^{94}Sr	$4.84 \times 10^{+4}$
Grouping total	$1.51 \times 10^{+6}$	Grouping total	$1.35 \times 10^{+6}$

Table 2.8. Decay heat contributions at shutdown from more than 800 fission product nuclides

FP contributors in order (groupings of nuclides)	LEU		HEU		Ratio of LEU/HEU cumulative decay heat
	Decay heat contribution of FP nuclide groupings (W)	Cumulative FP decay heat (W)	Decay heat contribution of FP nuclide groupings (W)	Cumulative FP decay heat (W)	
1–21	$1.51 \times 10^{+6}$	$1.51 \times 10^{+6}$	$1.35 \times 10^{+6}$	$1.35 \times 10^{+6}$	1.119
22–42	$1.01 \times 10^{+6}$	$2.52 \times 10^{+6}$	$8.84 \times 10^{+5}$	$2.23 \times 10^{+6}$	1.130
43–77	$1.17 \times 10^{+6}$	$3.68 \times 10^{+6}$	$1.02 \times 10^{+6}$	$3.25 \times 10^{+6}$	1.132
78–112	$6.94 \times 10^{+5}$	$4.38 \times 10^{+6}$	$6.06 \times 10^{+5}$	$3.86 \times 10^{+6}$	1.135
113–161	$4.15 \times 10^{+5}$	$4.79 \times 10^{+6}$	$3.53 \times 10^{+5}$	$4.21 \times 10^{+6}$	1.138
162–819	$2.31 \times 10^{+5}$	$5.02 \times 10^{+6}$	$1.95 \times 10^{+5}$	$4.41 \times 10^{+6}$	1.138

Assembled, fresh, HEU HFIR fuel elements have been experimentally determined to be subcritical by approximately three dollars (0.0228 in k-effective) when fully water reflected. There is some variability (up to about 20 cents) due to fuel manufacturing uncertainties. The MCNP (Ref. 16) model of the HEU core generated a k-effective of 0.983 when modeling this configuration. The assembled LEU core was modeled as fully water reflected, and a calculated k-effective of 0.951 was found. The result is consistent with lower BOL k-effective for the LEU core relative to the HEU core. Bred plutonium in the LEU cycle compensates, somewhat, for loss in reactivity due to burnup. K-effective for the outer element alone was calculated to be 0.758.

Control and safety integral element worth as a function of position was calculated using MCNP. The results of the calculations are shown in Fig. 2.7 for the LEU core (blue) and the current HEU core (red). For all the cases, the control and safety elements were in symmetric positions relative to the axial midplane of the core. The representation in Fig. 2.7 shows that the BOL critical configuration for the

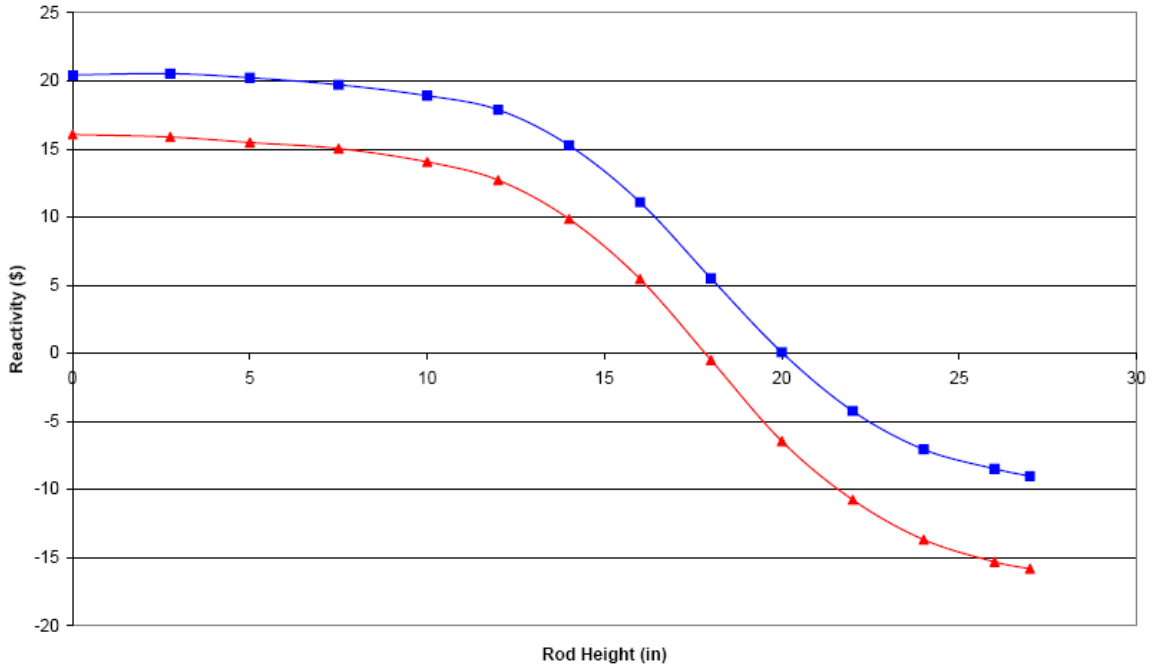

Fig. 2.7. Integrated control and safety element reactivity worth.

LEU core occurs with the control and safety elements withdrawn approximately 5 cm (2 in.) from their startup position for HFIR cycle 400 (red curve, HEU fuel). Careful inspection of the results reveals that the total integral worth of the control and safety plates, together, is slightly less for the LEU core than for the HEU core. The change in integral worth does not change the safety margin for the HFIR because the control/safety element worths assumed in the HFIR Safety Analysis Report are less than the calculated value for HEU shown in Fig. 2.7 (Ref. 17) and thus less than the LEU case.

2.2.3 Safeguards and Environmental Parameters

For the unconstrained thickness LEU case (85 MW and a burnup of 2210 MWd), the total amount of plutonium (Pu_{tot}) produced during one fuel cycle is 305.6 g. Approximately 279 g of ^{239}Pu (net) are generated. Very small amounts of other plutonium isotopes are created, as seen in Table 2.9. The $^{240}Pu/Pu_{tot}$ fraction is 6.6%.

In Table 2.10, the gamma source strength is compared for the HEU and LEU cores for some pertinent cooling times. The total source strength values are quite similar for the two cores. The methodology and computer program inputs used for both the decay heat and the gamma source strength/dose rate calculations are discussed in Appendix D.

Table 2.11 presents the gamma-ray dose rate calculations, from fission product sources, for the LEU and HEU cores 30 years after discharge from the reactor. Despite the similar gamma source strength tabulated in Table 2.11, the gamma dose rates for the LEU core and the inner fuel element and outer fuel element, separately, are less than 50% of the dose rate levels for the HEU core/components. The result is due to the large uranium content (hence higher density) of the LEU fuel relative to the HEU fuel. This effect reduces the "degree of self-protection" of the core, but the values in Table 2.11 are still within the current definition of self-protecting; especially since the maximum storage time for an element currently stored at HFIR is 12 years.

Table 2.9. Comparison of HFIR fuel isotopic content (kg) in LEU and HEU cores

Nuclide	HEU		LEU	
	BOL	EOL	BOL	EOL
^{235}U	$9.471 \times 10^{+1}$	$6.655 \times 10^{+1}$	$1.754 \times 10^{+1}$	$1.547 \times 10^{+1}$
^{238}U	5.554×10^{-1}	5.346×10^{-1}	$7.105 \times 10^{+1}$	$7.061 \times 10^{+1}$
^{238}Pu	1.666×10^{-5}	1.405×10^{-2}	1.666×10^{-5}	6.840×10^{-5}
^{239}Pu	9.005×10^{-6}	1.260×10^{-2}	9.007×10^{-6}	2.786×10^{-1}
^{240}Pu	3.200×10^{-3}	2.063×10^{-3}	3.200×10^{-3}	2.002×10^{-2}
^{241}Pu	3.002×10^{-7}	9.034×10^{-4}	3.002×10^{-7}	5.936×10^{-3}
^{242}Pu	8.557×10^{-6}	7.634×10^{-4}	8.557×10^{-6}	9.427×10^{-4}
^{252}Cf	2.252×10^{-7}	9.010×10^{-5}	2.252×10^{-7}	8.018×10^{-5}

Table 2.10. Gamma source strength (total photons/s) from fission products as a function of cooling time

HFIR core	0.5 year	1 year	5 years	30 years	100 years
HEU	$3.201 \times 10^{+16}$	$8.736 \times 10^{+15}$	$6.355 \times 10^{+14}$	$2.350 \times 10^{+14}$	$4.433 \times 10^{+13}$
LEU	$3.183 \times 10^{+16}$	$8.655 \times 10^{+15}$	$6.127 \times 10^{+14}$	$2.325 \times 10^{+14}$	$4.378 \times 10^{+13}$

Table 2.11. Dose rate (rem/h) at 30 years cooling time (in air at axial midplane, 1 m from outer surface of the source)

Source	LEU	HEU
Inner element	157.5	355.8
Outer element	243.2	596.0
HFIR core assembled	241.6	595.7

Isotopic concentrations for the HEU case and the LEU case are compared in Table 2.12 at BOL and EOL. The table contains the entire inventory of the HEU and LEU cores at 26 d (2210 MWd). The table entries, 125fp, 128fp, 149fp, and 141fp, are the lumped fission from ^{235}U, ^{238}U, ^{239}Pu, and ^{241}Pu, respectively. Note that the percentage change in curies for LEU-to-HEU conversion would be the same value as the percentage change in inventories.

Table 2.12. Isotopic inventory at EOL (2210-MWd/core) for HEU and LEU HFIR core

Nuclide	HEU inventory (kg)	LEU inventory (kg)	Difference % (L-H)/H	Nuclide	HEU inventory (kg)	LEU inventory (kg)	Difference % (L-H)/H
U234	8.766E–02	2.914E–01	232.42	Cs134	1.903E–03	1.399E–03	–26.48
U235	6.655E–00	1.480E+01	122.39	Cs135	2.851E–03	6.901E–03	142.06
U236	5.294E–01	6.061E–01	14.49	Nd143	3.392E–02	3.503E–02	3.27
U238	5.346E–01	7.060E+01	13106.14	Nd145	5.455E–02	5.446E–02	–0.16
Pu238	1.405E–03	6.840E–05	–95.13	Nd147	1.537E–02	1.545E–02	0.52
Pu239	1.260E–02	2.786E–01	2111.11	Pm148	2.481E–04	2.182E–04	–12.05
Pu240	2.063E–03	2.002E–02	870.43	Pm148m	1.626E–04	2.156E–04	32.60
Pu241	9.034E–04	5.936E–03	557.07	Pm149	2.168E–03	2.125E–03	–1.98
Pu242	7.634E–04	9.427E–04	23.49	Sm150	1.289E–02	1.256E–02	–2.56
H	2.493E+02	2.493E+02	0.00	Sm151	1.233E–03	2.548E–03	106.65
O	1.997E+03	1.996E+03	–0.05	Sm152	7.573E–03	7.026E–03	–7.22
Si	3.842E–01	1.052E–00	173.82	Eu155	1.151E–04	1.541E–04	33.88
Fe	6.762E–01	6.643E–01	–1.76	Eu153	4.992E–00	4.991E–00	–0.02
Cu	3.851E–01	3.783E–01	–1.77	Eu154	1.161E–03	1.087E–03	–6.37
Mn55	1.447E–01	1.421E–01	–1.80	Pm147	1.354E–02	1.427E–02	5.39
Mg	7.706E–01	7.570E–01	–1.76	Pr143	4.504E–02	4.486E–02	–0.40
Cr	3.372E–01	3.313E–01	–1.75	Sm149	3.858E–04	1.080E–03	179.94
Ti	1.445E–01	1.420E–01	–1.73	Sm153	6.703E–04	5.568E–04	–16.93
Al	1.623E+02	1.767E+02	8.87	Tc99	5.814E–02	5.833E–02	0.33
Am241	4.695E–05	6.585E–05	40.26	Zr93	5.861E–02	5.763E–02	–1.67
Cm244	6.126E–02	6.182E–02	0.91	Ce141	6.160E–02	6.128E–02	–0.52
Am243	1.304E–03	1.366E–03	4.75	B10	1.858E–04	5.370E–04	189.02
Cm245	8.464E–04	8.943E–04	5.66	B11	1.248E–02	1.248E–02	0.00
Cm246	4.714E–02	4.715E–02	0.02	C	4.210E–03	4.210E–03	0.00
Cm247	1.360E–03	1.378E–03	1.32	Np237	1.536E–02	6.311E–04	–95.89
Cm248	8.266E–03	8.257E–03	–0.11	Np238	0.000E+01	1.268E–05	–
Cf252	9.010E–05	8.018E–05	–11.01	Np239	0.000E+01	5.334E–02	–
Cm242	4.125E–04	4.063E–04	–1.50	Eu151	4.537E–00	4.537E–00	0.00
Bk249	5.894E–05	6.178E–05	4.82	Ta181	9.933E–00	1.162E+01	16.98
Cf249	4.182E–07	4.904E–07	17.26	Ta182	2.273E–02	2.675E–02	17.69
Cf250	4.057E–05	4.172E–05	2.83	Hf	0.000E+01	0.000E+01	–
Cf251	1.260E–05	1.318E–05	4.60	Be	8.014E+02	8.014E+02	0.00
Cf253	2.238E–06	1.731E–06	–22.65	Kr85	2.378E–03	2.320E–03	–2.44

Table 2.12. (continued)

Nuclide	HEU inventory (kg)	LEU inventory (kg)	Difference % (L-H)/H	Nuclide	HEU inventory (kg)	LEU inventory (kg)	Difference % (L-H)/H
Es253	3.761E–07	2.952E–07	–21.51	Sr89	3.506E–02	3.416E–02	–2.57
Cm243	1.004E–05	9.551E–06	–4.87	Y91	4.516E–02	4.415E–02	–2.24
Am242m	4.077E–07	5.675E–07	39.20	Ru106	4.269E–03	5.336E–03	24.99
Pu243	2.502E–06	2.671E–06	6.75	I131	1.497E–02	1.502E–02	0.33
Am242	4.744E–06	5.569E–06	17.39	Ce144	7.604E–02	7.490E–02	–1.50
Mo	5.638E–02	9.886E–00	17434.59	Xe131m	1.501E–04	1.503E–04	0.13
Ru101	5.037E–02	5.044E–02	0.14	Zr95	5.332E–02	5.253E–02	–1.48
Ru103	2.483E–02	2.576E–02	3.75	Nb95	6.626E–03	6.547E–03	–1.19
Rh103	5.572E–03	5.900E–03	5.89	Rh103m	2.463E–05	2.555E–05	3.74
Rh105	4.185E–04	6.695E–04	59.98	Pr144	3.203E–06	3.155E–06	–1.50
I135	1.283E–03	1.275E–03	–0.62	125fp	7.164E–01	6.842E–01	–4.49
Xe131	2.064E–02	2.112E–02	2.33	128fp	8.563E–05	9.942E–03	11510.42
Xe133	2.381E–02	2.408E–02	1.13	149fp	1.253E–03	1.144E–02	813.01
Xe135	4.931E–05	1.376E–04	179.05	141fp	5.116E–04	6.192E–04	21.03

2.2.3.1 Thermal-hydraulic parameters

Results from the HFIR steady state heat transfer code (HSSHTC, see Refs. 1, 18) for various times in the HEU fuel cycle are contained in Ref. 1 and reprinted below as Table 2.13 (note English units used in Ref. 1). These calculations, as well as diffusion theory calculations for the unconstrained thickness LEU cycle indicate that limiting thermal-hydraulic conditions (meaning minimum margin to

Table 2.13. Burn-up-dependent heat transfer data—incipient boiling criteria—for HEU fuel[a]

Time into cycle	BOC	1.014 d	11.57 d	22.72 d	25.0 d
Limiting power level, MW	110.63	120.89	116.51	116.34	120.35
Operating power level, MW	85.1	93.0	89.6	89.5	92.6
Limiting heat flux:					
Location, fuel element (*i*,*j*)	Outer (3,29)	Inner (5,29)	Inner (5,29)	Inner (5,29)	Outer (4,29)
Heat flux, Btu/h-ft^2	2.80E+6	2.81E+6	2.79E+6	2.87E+6	2.70E+6
Bulk water temperature, °F	274	276	278	275	286
Surface temperature, °F	422	422	422	422	422
Heat transfer coefficient, Btu/h-ft^2, °F	18,920	19,250	19,375	19,525	19,850
Flow rate, 1b/s-in. width	0.7473	0.6754	0.6468	0.6421	0.6684
Pressure, psia	264	264	264	263	263
Maximum hot streak outlet bulk water temperature:					
Location, fuel element (*i*)	Outer (4)	Outer (4)	Outer (4)	Outer (4)	Outer (4)
Magnitude, °F	275	285	282	282	286
Flow rate, lb/s-in. width	0.7027	0.6948	0.6650	0.6594	0.6684
Minimum flow rate:					
Location, fuel element (*i*)	Inner (4)	Inner (5)	Inner (5)	Inner (5)	Inner (5)
Magnitude, lb/s-in. width	0.6848	0.6754	0.6468	0.6421	0.6530
Bulk water temperature at outlet, °F	271	276	278	275	273

[a]Reactor conditions based on 130°F coolant inlet temperature and 368-psig reactor pressure (equivalent to 375-psia fuel assembly inlet pressure). Coolant inlet temperature uncertainty factor U_6 is set to 1.0. Locations (*i*,*j*) defined in Ref. 1.

incipient boiling) occur at beginning-of-cycle (BOC). Consequently, only BOC MCNP-derived calculations are reported for the LEU cycle in Table 2.14. For the convenience of the reader, HEU data from Table 2.13 are converted to SI units and compared to the LEU cycle in Table 2.14. The maximum fuel temperature—meaning the maximum temperature in the U-10Mo region inside a plate—was calculated using the HEATING module of the SCALE system (see Appendix E).

2.3 STACKS OF MONOLITHIC FOILS

Section 3.2.1.2 of Ref. 1 identifies a case for study that is based on stacking minimum-thickness foils in a pyramidal shape to achieve, in a stepwise fashion, a graded fuel meat profile. In mid-2006, the RERTR program identified a minimum obtainable foil thickness of 25.4 μm (1 mil). At that time, the program management decided there was no need to consider a "stacked foils" case because the "stair-steps" in the profile would be the same, when modeled as discrete regions in the neutronics analysis computer programs, as an approximation to a continuous profile. The results of the neutronics calculations performed for fuels with 25.4-μm increments in height would be indistinguishable from neutronics calculations performed with approximations to continuously graded fuel. With program management approval, "stacked foil" cases were deleted from the LEU studies.

Table 2.14. LEU and HEU beginning-of-cycle heat transfer data—incipient boiling criteria

Parameter	LEU	HEU	% change [100*(LEU-HEU)/HEU]
Reactor power (MW)	110.4	110.6	~0
Location of incipient boiling fuel element; along fuel zone, down fuel zone (cm)[a]	Inner, 2.40, 50.8	Outer, 0.19, 50.1	–
Heat flux, MW/m^2	8.46	8.83	–4.19
Bulk water temperature, °C	135	134	0.75
Clad surface temperature, °C	212	217	–2.30
Maximum temperature in fuel meat, °C	224	–	–
Heat transfer coefficient [W/(m^2*K)]	102,211	107,352	–4.79
Flow rate at this location (kg/s-cm width)	0.1284	0.1335	–3.82
Pressure at this location, kPa	1,643	1,820	–9.73
Incipient boiling maximum hot streak outlet bulk water temperature[b]			
Fuel element, location along plate (cm)	Inner, 1.175	Outer, 0.627	–
Magnitude, °C	137	135	1.48
Flow rate (kg/s-cm width)	0.1242	0.1255	–1.04
Incipient boiling conditions at outlet location of minimum flow rate			
Fuel element, location along plate (cm)	Inner, 1.175	Inner, 0.691	–
Outlet bulk water temperature, °C	137	133	3.01
Flow rate, (kg/s-cm width)	0.1242	0.1223	1.55

[a]Top, inside (toward central target) edge is 0, 0. Positive z direction is down the fuel. Values are the centerpoints of the node, not actual location of peak.

[b]Hot streak may be at different location than hot spot due to pressure differences along plate.

3. DISPERSION FUELS

Dispersion fuel consists of minute U-10Mo fuel particles, of approximately the same diameter as U_3O_8 particles in the current HEU fuel, intermixed with a silicon-stabilized aluminum powder. Because it is not currently known if a diffusion barrier is required or desired, in one case, the dispersion particles are assumed to have no diffusion barrier coating, only spherical U-10Mo particles (uncoated case). In the second case, a diffusion barrier coating (natural Nb) encases the U-10Mo particles (coated case). The effective uranium density of the uncoated dispersion fuel is 0.50 of the monolithic U-10Mo. The uranium density of the coated fuel is further reduced—0.41 times the monolithic U-10Mo density.

The monolithic studies showed that the fuel loading required to achieve equivalent cycle length and burnup as the current HEU cycle is about 17 kg of ^{235}U. This parameter is generally independent of fuel form—monolithic or dispersion. However, the reduced uranium density in the dispersion fuels leads to the thickness of the fuel meat being much greater for dispersion fuels than for monolithic fuels.

For both coated and uncoated cases, it was not possible to achieve the same level of performance as found in monolithic fuels. Achieving desired cycle length compromised operating power. Achieving maximum operating power compromised cycle length. Combinations of operating power and cycle length are shown in Table 3.1.

Table 3.1. Operating conditions for dispersion fuel cycles

Case	Operating power (MW)	^{235}U loading (kg)	Cycle length (MWd)
Current, HEU	*85*	*9.4*	*2210*
Coated LEU, max. op. power	88	10.9	935
Coated LEU, max. cycle length	40	17.1	2805
Uncoated LEU, max. op. power	85	13.2	1870
Uncoated LEU, max. cycle length	77	17.5	2465

In the “maximum operating power” (max. op. power) option, the shape of the ^{235}U distribution was assumed to be the same as the unconstrained minimum-thickness monolithic fuel case with the peak thickness expanded to 688 μm (27.1 mils), the same as the current HEU fueled core. This methodology allowed for maximum ^{235}U loading under the constraint of the previously identified optimum fuel distribution. This methodology is not guaranteed to yield the maximum operating power (radial peaks could be reduced by shifting fuel toward the center of the plate) but likely yields an operating power close to the maximum due to axial end peaking likely being the principal factor in establishing maximum operating power. For the “maximum cycle length” option, the fuel zone is ungraded and filled to the maximum thickness specified in Ref. 1—688 μm.

Table 3.1 presents a number of important effects and behaviors for HFIR cores dependent on the total ^{235}U loading and the fraction of the ^{235}U in the inner fuel element (IFE). The current HFIR HEU core has 27.5% of its ^{235}U in the IFE. By comparison, the LEU monolithic fuel core has 20.6% of its ^{235}U in the IFE. The reduced ^{235}U fraction in the IFE is a result of fuel grading designed to satisfy fuel power density and coolant enthalpy constraints. As mentioned above, the coated and uncoated LEU cases designed for maximum operational power have grading profiles similar to the LEU monolithic case, in order to satisfy all power density, fuel temperature, and coolant enthalpy limits. As a consequence, due to the reduced ^{235}U density of the dispersion fuels, the ^{235}U loading of the two cases is 10.9 kg and 13.2 kg, respectively. The fraction of ^{235}U in the IFE is 20.6% for both cases. These

cases meet or exceed the current HFIR HEU core total power level of 85 MW, but the cycle lengths are considerably shorter than for the HEU core, as seen in Table 3.1.

To increase the cycle length of these two dispersion fuel designs, the ^{235}U loading was substantially increased to approximately the same total loading as the LEU monolithic U-10Mo core. Because the coated dispersion fuel has a relatively low ^{235}U density, it was necessary to completely fill the available 27.1-mil thickness in the fuel plates for both the IFE and OFE, as seen in Table 3.2. This completely removes the benefit of fuel grading for this case, but also increases the ^{235}U fraction in the IFE to 33.8%. The removal of the fuel grading results in the required reduction in core operational power level to 40 MW for peak power density and coolant enthalpy considerations. However, the relative shift of ^{235}U to the IFE results in a significant increase in the cycle length, because the higher thermal neutron flux levels in the IFE results in higher importance, and core reactivity, for the fissile uranium "moved" to the IFE from the outer fuel element.

The uncoated dispersion fuel case was adjusted to have a total loading of 17.1 kg of ^{235}U. The uncoated dispersion fuel, with its greater ^{235}U density, still allowed for some fuel grading (as seen in Table 3.3). The net effect is that the IFE contains 26.6% of the ^{235}U. The fuel grading was sufficient to

Table 3.2. Coated LEU dispersion fuel profile and current HEU profile

Distance along inner element plate (cm)	Thickness of fuel meat (mils)			Distance along outer element plate (cm)	Thickness of fuel meat (mils)		
	LEU				LEU		
	Maximum operating power	Maximum cycle length	HEU		Maximum operating power	Maximum cycle length	HEU
0.252	5.0	27.1	10.2	0.191	9.1	27.1	15.3
0.448	5.1	27.1	11.6	0.216	10.2	27.1	15.6
1.203	6.0	27.1	15.5	0.395	15.7	27.1	16.9
2.439	9.9	27.1	20.5	1.134	22.6	27.1	23.0
3.811	12.7	27.1	24.4	2.256	27.1	27.1	27.1
5.314	13.3	27.1	24.6	3.449	26.1	27.1	25.5
6.969	11.1	27.1	21.5	4.655	19.1	27.1	20.7
7.985	8.3	27.1	18.6	5.908	12.2	27.1	14.7
8.091	8.1	27.1	18.3	6.731	10.2	27.1	11.5

Table 3.3. Uncoated LEU dispersion fuel profile and current, HEU profile

Distance along inner element plate (cm)	Thickness of fuel meat (mils)			Distance along outer element plate (cm)	Thickness of fuel meat (mils)		
	LEU				LEU		
	Maximum operating power	Maximum cycle length	HEU		Maximum operating power	Maximum cycle length	HEU
0.252	5.0	7.3	10.2	0.191	9.1	16.2	15.3
0.448	5.6	7.9	11.6	0.216	10.1	17.8	15.6
1.203	5.9	10.4	15.5	0.395	15.6	26.6	16.9
2.439	9.8	16.1	20.5	1.134	22.6	27.1	23.0
3.811	12.7	21.3	24.4	2.256	27.1	27.1	27.1
5.314	13.3	22.9	24.6	3.449	26.0	27.1	25.5
6.969	11.1	19.3	21.5	4.655	19.1	25.7	20.7
7.985	8.3	15.1	18.6	5.908	12.1	14.9	14.7
8.091	8.2	14.7	18.3	6.731	10.1	12.9	11.5

allow for an operational power level of 77 MW, while satisfying the power density and coolant enthalpy constraints. The cycle length for this uncoated dispersion fuel case is longer than the reference HEU core 26-d (at full power) cycle, which is equivalent to 2210 MWd.

3.1 COATED PARTICLES

Fuel meat thickness profiles for the coated particle cases noted in Table 3.1 are provided in Table 3.2. Because the maximum cycle length case has a flat profile, it is conceptually possible that the fuel meat thickness could be extended to 762 μm and the aluminum filler region eliminated from the fuel plate.

3.2 UNCOATED PARTICLES

Fuel meat thickness profiles for the uncoated particle cases noted in Table 3.1 are provided in Table 3.3. As for the coated particle cases, since the maximum cycle length case has, essentially, a flat profile, it is conceptually possible that the fuel meat thickness could be extended to 762 μm and the aluminum filler region eliminated from the fuel plate. Nevertheless, the case description provided in Table 3.3 already yields an unacceptable operating power and a cycle length that exceeds the current HEU fuel cycle.

3.3 CONCLUSIONS REGARDING DISPERSION FUELS

Though none of the dispersion cases resulted in a fuel cycle equivalent to the current HEU cycle (in terms of operating power and cycle length), the uncoated, maximum operating power case was sufficiently close to the performance achieved with the monolithic fuels to merit additional study. RERTR program management have requested additional studies of this fuel option during FY 2007. Two of the assumptions in Ref. 1 are to be modified for the succeeding studies. The fuel form will be U-7Mo, and the packing fraction will be assumed to be 0.55. Both of these assumptions will result in higher fuel loading per unit thickness and therefore potentially lead to longer cycle length. Refinements in radial grading could potentially increase, slightly, the operating power. To the extent possible, increasing the ^{235}U fractional loading in the inner fuel element will have the desirable effect of increasing the core cycle length.

Though one-dimensional grading studies will be continued in FY 2007, dispersion fuels are not amenable to two-dimensional grading. Achieving an increase in power above 85 MW in order to maintain the performance of the HFIR at its current levels appears to require two-dimensional grading.

4. ENGINEERING/ECONOMIC ASSESSMENT

Analyses presented earlier in this study have shown that a same-dimensions LEU replacement for the current HEU core, in terms of performance, has not been found. Nevertheless, based upon the results of the neutronic and thermal-hydraulic analyses for the unconstrained minimum thickness LEU core design, an overall engineering assessment was conducted under the assumption than an acceptable fuel can be developed to meet all the requirements stated in Ref. 1. The assessment was conducted using the Delphi technique and uses a "success-driven" schedule, that is, the assumption is made that no unforeseen problems occur during the lifetime of the project. Managers in the ORNL Research Reactors Division responsible for operations, safety, fabrication, and environmental impact were consulted for cost and scheduling estimates for changes to the HFIR site to accommodate an LEU fuel cycle. The result of these discussions was a preliminary cost estimate of the required capital improvements, safety analysis updates, changes to Technical Safety Requirements, procedural modifications, and required training to support the implementation of core conversion.

The assessment was limited to operations at the HFIR site (7900 area of ORNL) because the RERTR program has funded other organizations to develop fuel production capabilities and fuel plate and fuel element fabrication capabilities. Consequently, these fuel production costs were excluded from this study. The cost of 19.75% enriched uranium was also not considered. Currently the HFIR annual budget includes payment for the processing of HEU into U_3O_8 but not for the HEU itself. Possible sources of LEU include down-blending HEU or the purchase of the material from an enrichment facility. Either would incur costs that are not a part of the HEU fuel cycle. Likewise, an assessment of the acceptability of uranium-molybdenum for long-term storage of spent fuel was not performed because that operation will not be at the ORNL site. An assessment was not made of the capital improvements required to HFIR to run the reactor with the LEU fuel at 100 MW to recover the flux lost to the beam tubes due to converting from HEU to LEU.

The conclusions of the assessment follow (costs given in each bullet are in constant 2006 dollars):

a. HFIR operations require that approximately 40 cores be stored in inventory due to the short fuel cycle length and the relatively long fabrication time. HEU cores are stored at the Y-12 National Security Complex in a specially designated HEU storage area. LEU cores will likely require the construction of a new storage facility at the HFIR site unless storage can be accommodated at the fuel fabrication site with just-in-time delivery to HFIR. Since HFIR is authorized to operate for another 40 years at the current power level, the lifetime of a new storage facility should be the same. Currently, the cost of fresh fuel receipt, storage, and transportation to the HFIR site is $85,000 per year. A new storage facility at the HFIR site will be a security category 2 or 3 level facility and have an expected capital cost of $25M ($25,000,000 in FY 2006 dollars). Operating costs for the facility will be $300,000 per year. The annual update to the Safety Analysis Report for the facility would be $100,000 per year. The facility will have to be equipped with 80 storage containers for a total cost of $800,000. A new, fresh fuel shipping container for transport from the fuel fabricator to HFIR will be needed (since shipment will no longer use SST transport with LEU fuel) with an estimated cost of $5M. The time to design, build, license, and prepare an environmental impact statement is estimated to be 4 years. An alternative plan would be to provide new storage capacity at the fuel fabricator with just-in-time delivery to HFIR. The cost of such a facility has not been estimated but is judged likely to be comparable to providing a new storage facility at HFIR.

b. Due to the increased weight of the LEU core relative to the HEU core, two new tools for fuel transfer from the storage building to the reactor building will be required. Estimated cost is $250,000, and time-to-completion is 6 months.

c. Three new tools for fresh fuel handling operations inside the reactor building will be needed (inner element tool, outer element tool, and combination tool). Estimated cost is $1M, and time-to-completion is 1 year.

d. Due to the increased weight of the LEU core relative to the HEU core, structural analyses will have to be conducted on the core components (including the core stack) and must include seismic analyses. Estimated cost is $1M, and time-to-completion is 1 year.

e. New analyses will be conducted for the spent fuel storage area including structural, criticality safety, and decay heat studies. Both the floor and storage rack structural analyses will have to be performed. Currently, spent fuel storage operations at HFIR are limited to approximately 90% of capacity by inadequate structural analyses. Estimated cost is $4M, and time-to-completion is 1 year.

f. Spent fuel assemblies are stored in cadmium jackets in the newest HFIR storage array. A new, jacketed assembly tool will be required for LEU. Estimated cost is $600,000, and time-to-completion is 1 year.

g. Changing regulations have required that the safety basis for the existing spent fuel shipping cask be reviewed and updated periodically. Considering past reviews, it is likely that a new cask will be required for LEU and therefore new analyses: criticality safety, thermal, structural. A "drop analysis" will be needed and the cask must be licensed by the Department of Transportation. The estimated cost is $15 M, and the time to completion is 8 years. Training will be required for the new cask/handling equipment/lifting tools. Estimated cost is $500,000, and time-to-completion is 3 months.

h. During the first several years of operation with LEU, both HEU and LEU elements will be in the spent fuel storage array. Safety studies must be performed for various mixed, interim configurations (criticality safety, structural, thermal analyses). Estimated cost is $1.2M, and time-to-completion is 18 months.

i. Structural tests of "production" fuel plates and elements supplied from the fabricator will be required because the fuel core is U-10Mo alloy rather than U_3O_8/Al. The estimated cost is $5M, and the time-to-completion is 3 years.

j. Changes to the fuel meat region of the plates will constitute a "major modification" in accordance with DOE Order 430.1b. The conversion is assumed to be done under DOE project management guidelines—DOE P 413.1 Program Management Policy (M 413.3-1 is manual, the Order is 413.3-A). This procedure imposes scheduling requirements.

k. A specification for the U-10Mo foil production operation will have to be written. The estimated cost is $200,000, and the time-to-completion is 6 months. The specification will be needed to license the fresh fuel storage and shipping containers.

l. A specification for the fabrication of the fuel plates and elements must be written. The estimated cost is $400,000, and the time-to-completion is 1 year. The specification will also be needed to license the fresh fuel storage and shipping containers.

m. Chapter 4 of the Safety Analysis Report will require extensive revision. New physics/thermal hydraulic *certified* analyses; reactivity estimates, radiation source terms, and estimates of thermal operating conditions must be developed. Estimated cost is $1.5M, and time-to-completion is 2 years.

n. Reactor core power distributions will have to be measured in critical experiments. These measurements will have to be done at the HFIR facility since there are no other critical facilities capable of such measurements in the United States. It is assumed that after irradiations with LEU are performed, the reactor returns to HEU operation while test data are analyzed and documents prepared. Because the HFIR facility will not be operational for scattering experiments during this time that LEU critical experiments are conducted, the cost of this task is estimated at $15M with an additional $1M for analyses and documentation. Calendar time for this task is estimated to be 1 year.

o. Those portions of the Safety Analysis Report impacted by the new structural analyses will be updated. Estimated cost is $200,000, and time-to-completion is 6 months.

p. Chapter 15, accident analyses, of the Safety Analysis Report will need extensive revision. Analysis methodologies will need upgrades, $600,000 and 1 year for upgrade and certification for migration to RELAP5, MOD3.3; $600,000 and 2 years for upgrade and certification of MELCOR.

q. The change in the differential control element worth due to conversion (though this appears to be very slight) will lead to changes in accident sequences. The estimated cost of analyses is $15M, and the time-to-completion is 5 years. A previous revision similar in scope extended from 1987–1992 at a cost of $7M.

r. Because the plutonium content of LEU fuel is significantly greater than HEU, escape of plutonium particulates from a damaged fuel plate could lead to dose consequences much more severe than HEU. New emergency plans will be required, possibly due to increased actinide hazard, but certainly because of the presence of a new fresh fuel storage building on site. Estimated cost is $2M, and time-to-completion is 2 years.

s. For Technical Safety Requirements, new SCRAM set-points must be established because the transient response for LEU will be different than for HEU. Instrumentation and controls must be examined and adjusted as needed. It is not clear that the operation of the reactor could easily switch from HEU to LEU and return to HEU as assumed above in developing a cost estimate for the reactor physics tests. Due to the increase in decay heat rate at shutdown for LEU relative to HEU (see Appendix D), a change to the TSRs would likely be required – likely three pony motor pumps would be required for reactor operation and two during shutdown. Estimated cost is $1M, and time-to-completion is 3 years.

t. DOE procedures approve projects in five phases—CD0, 1, 2, 3, 4. Experience shows that a 6-month regulatory approval time occurs following each request for approval for a phase. A similar situation existed when the HFIR SAR was submitted in October 1992 and was not approved until April 1998; however, consistent with the assumption of a “success-driven” schedule, a 6-month time frame is assumed for the regulatory review phases.

u. The sum of the above costs constitute the “Base Project.” Appropriately selected inflation and contingency factors must be applied to this analysis. To properly escalate the costs, a reference project schedule was developed and is shown in Fig. 4.1.

A contingency calculation at this point in the project could not be performed using formal risk analysis, mainly due to the lack of “input” uncertainty data on each of the major project elements. Instead a deterministic method outlined in the January 2004 “USDOE Cost Estimating Guide” was used. It assigns an overall project contingency based on the level of cost estimating applied and the purpose of the estimate. (The characteristics are defined in five classes by the American Association of Cost Engineers; with class 1 being most detailed and class 5 as least detailed.) This estimate falls between levels 4 (Study or Feasibility) and 3 (Budget Authorization). The accuracy ranges listed for each estimate class in the table in the DOE document suggested that a 30% general contingency applicable to all project elements is appropriate at this point.

An escalation factor of 2.3% per year is assumed. This is the value for years 2007 and beyond suggested by DOE’s Office of Engineering and Construction Management in the table on their website: http://oecm.energy.gov/cost_estimating/2004Rates.pdf.

This contingency was uniformly applied to all of the cash flows before escalation. Cash flows were derived by assigning the activity funding (listed in each of these bullets a., b., etc.) using the schedule shown in Fig. 4.1. Table 4.1 shows the annual cash flows (including contingencies and escalation) with annual cash flows presented graphically in Fig. 4.2.

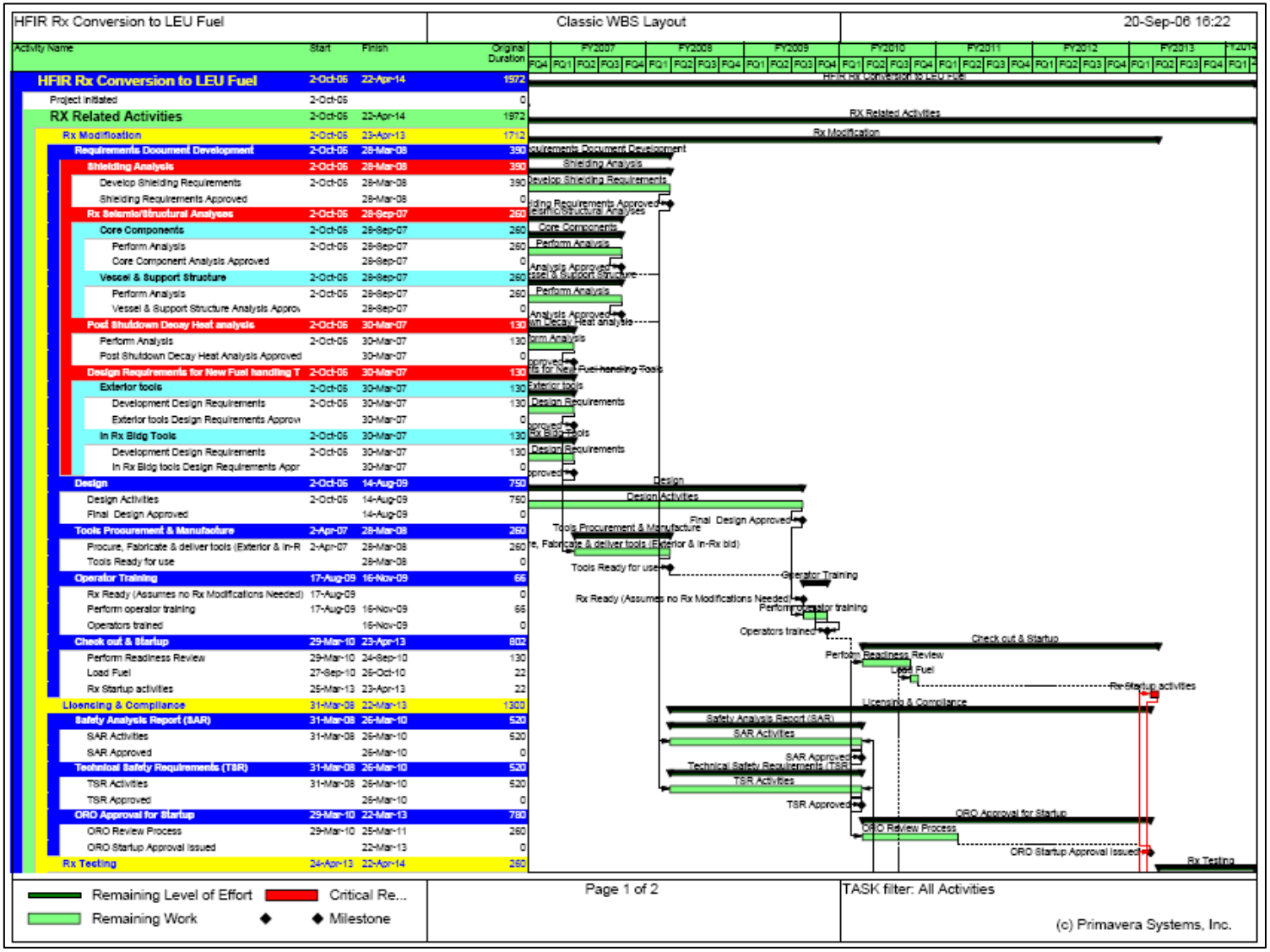

Fig. 4.1. Derived project schedule to meet operation date of October 1, 2014.

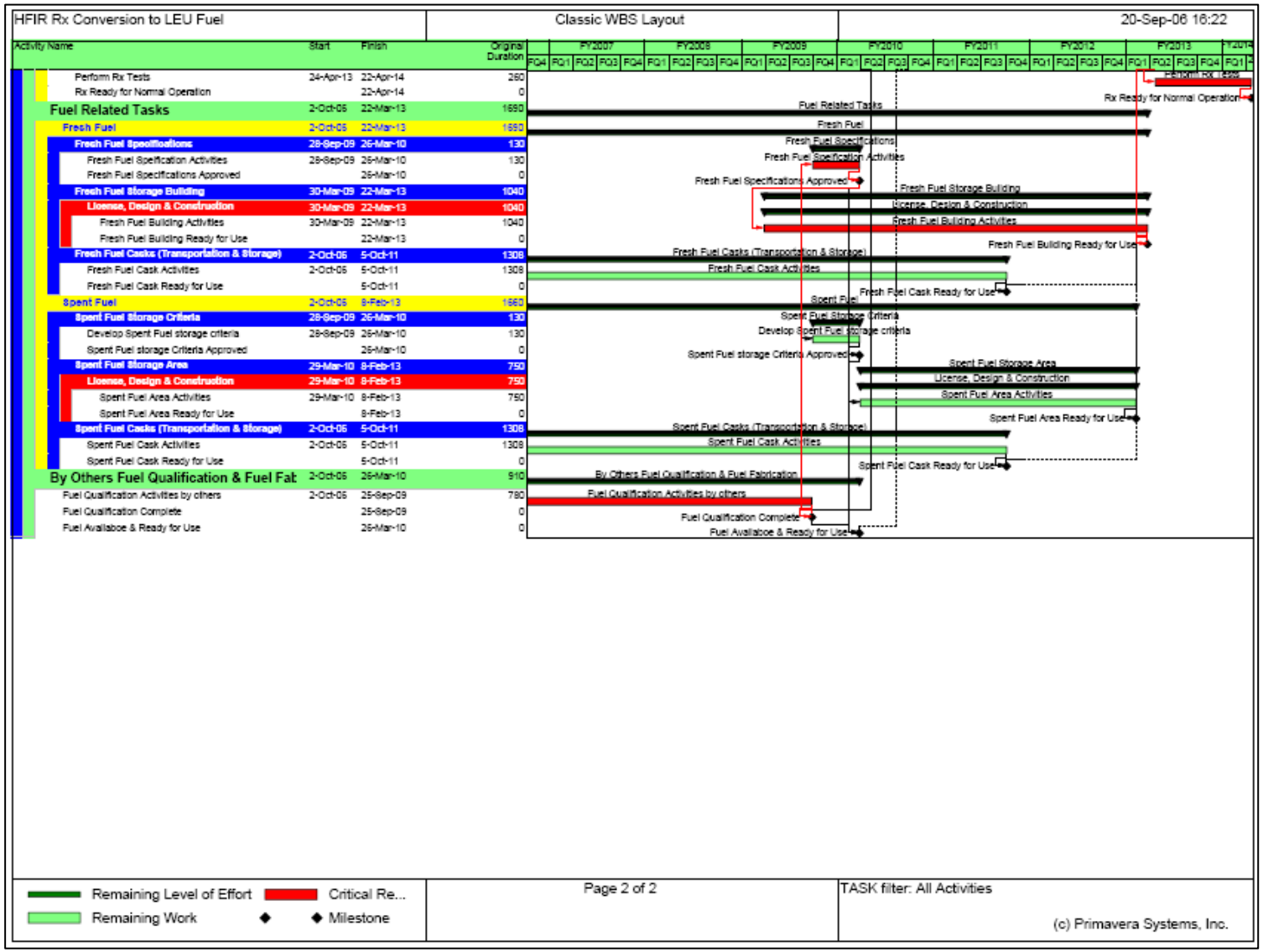

Fig. 4.1. (continued).

Table 4.1. Annual cash flow for HFIR site (7900 area) LEU project

Fiscal year	Cost (K$)
2007	3,491
2008	10,918
2009	11,900
2010	22,567
2011	34,666
2012	20,712
2013	26,066
2014	11,539
Total	141,858

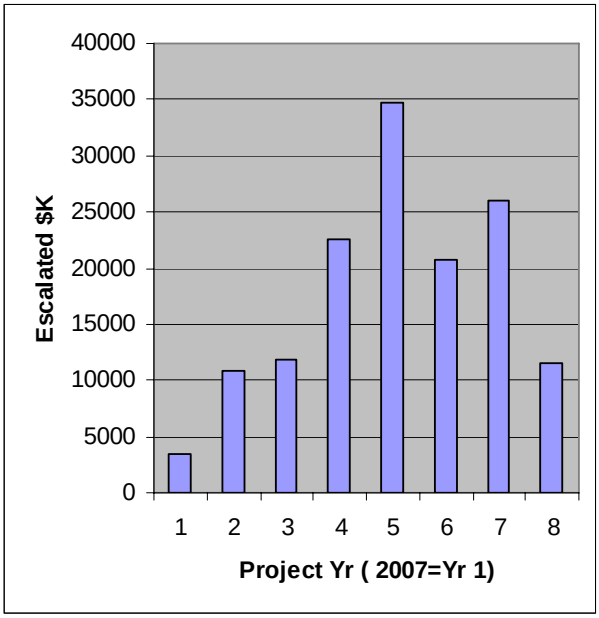

Fig. 4.2. Cash flow by year for HFIR site (7900 area) for LEU project.

While gathering these cost data, HFIR staff provided some pertinent information regarding the feasibility of increasing the HFIR operating power to 100 MW. The refrigeration system for the HFIR cold source was designed for a reactor operating power of 100 MW. The determination of whether this goal was achieved will be known at the startup of the cold source, currently scheduled for December 2006. While not included in this study, if the flux penalty for LEU could be mitigated by an increase in reactor power, then an assessment should be conducted as to the adequacy of the refrigeration system for the HFIR operation at >85 MW. The reactor cannot be operated without the cold source also being operational. If a new refrigeration unit is required for operation at 100 MW, the cost could be up to $30M with an additional $500,000 required to remove and dispose of the existing system and install the new system. Time-to-completion is estimated at 3 years.

The conclusion of this assessment was that the cost of the "Base Project" LEU conversion activities at the HFIR site *if an acceptable fuel can be fabricated* would exceed $125M in constant dollars and $140M in escalated dollars. The estimated times for conducting the various tasks to convert the HFIR site lead to the conclusion that, if LEU fuel will be available to be loaded in 2014, then the conversion of the HFIR site should begin in fiscal year 2007. The necessary completion of safety analysis report preparation by the end of fiscal year 2009 would require the completion of all fuel development activities prior to date. Such a requirement is not consistent with the current RERTR fuel development program schedule.

5. IMPLICATIONS OF FY 2006 STUDIES FOR THE CONVERSION OF HFIR TO LEU FUEL

1. The fuel thickness in the inner element does not vary significantly as a function of distance along the plate. Thus, the presence of boron in the filler region of the plate does not impact the power distribution because there is no spatial variability in the boron distribution. The boron does seem to act to shift the power from the inner to the outer element, but it is not clear whether the effect could be achieved via other design options.

2. The axial power peaks, especially at the base of the fuel plate (coolant exit) are driving factors in limiting the operating power for the LEU cycle. Because the ^{235}U loading in the LEU core must be twice the value of the HEU core to achieve the same cycle length, the LEU cores studied can never achieve lower local power densities than the HEU core regardless of the effort spent in grading the fuel (but it can be minimized). With one-dimensional grading, the average ^{235}U density along the lower edge will always be approximately twice the value of the HEU core. The flux in that region will be relatively insensitive to the ^{238}U content because it will always be thermalized due to the presence of water below the fuelled region of the core. These two factors mandate that the local power density somewhere along the lower edge of the LEU cores studied will always be higher than the maximum local power density along the lower edge of the HEU core.

3. For the unconstrained thickness case, the minimum fuel thickness is 84 μm (3.3 mils) with a reported manufacturing uncertainty of 25.4 μm (1 mil). This results in a 30% uncertainty in the fuel distribution which exceeds the currently assumed value in the steady-state heat transfer calculations (per Ref. 1) of 12%. Maintaining the current HFIR criterion of 12% would mean that the uncertainty in the U-10Mo thickness would have to be 10 μm (0.4 mil).

4. Given that LEU designs have been found that permit operation of HFIR at the currently authorized operating power of 85 MW and maintain the existing cycle length, the 15% penalty in flux to the cold source is an inherent property of LEU fuel. The Executive Director of HFIR has reviewed these FY 2006 LEU studies and concluded:

   > *We cannot afford to compromise on reactor performance—what we have in flux we need. We have no problem converting to LEU provided the above is met and someone is capable of paying the cost without significant mission impact. Our current studies are inconclusive but we do believe that a technology breakthrough will be required. We are not terribly optimistic but it is too early to say we can or cannot meet a 2014 conversion.*

6. RECOMMENDED STUDIES FOR FY 2007

The proposed work in FY 2007 in the HFIR LEU conversion feasibility project will build upon and extend the results and scope of the assessment of the HFIR LEU core options. The goal of the studies is to find a design that results in no degradation to the performance parameters for HFIR and identifying the cost and schedule at the HFIR site of implementing the design. These studies are consistent with the goals established by the Executive Director of HFIR.

The reactor analysis effort is organized into four areas: further studies of the one-dimensionally graded profiles (radial), studies of two-dimensionally graded profiles (radially and axially), development in analysis methodologies that will reduce conservatism in both one- and two-dimensional (1-D and 2-D) methodologies, and program management costs such as report preparation, travel, and advisory/review committee meeting participation. Some additional details for these four areas of study are shown in Table 6.1

The current core design and LEU evaluation is based on a 1-D radial grading of the fuel. At the request of the RERTR program management, during FY 2007, additional studies of uncoated, dispersion fuel will be conducted to determine if the HFIR operating power for this fuel could be

Table 6.1. Reactor analysis activities proposed for FY 2007

Area of study	Task ID	Subtask description
1-D graded fuels	Monolithic	Boron in aluminum end plate Transient analyses of reference design Determine maximum cycle fluence
	Dispersion	Increased volume fraction (0.55) for uncoated fuel and change of fuel type to U-7Mo; include boron in aluminum end plate if positive benefit
2-D graded fuels	Monolithic	Develop grading profile Transient analyses of reference design Determine maximum cycle fluence
Economic/engineering assessment	Conversion to power >85 MW; both 1-D and 2-D fuels as appropriate	Similar study as Chap. 4 but identifies cost/schedule for increasing HFIR power so performance meets/exceeds current value
Methods/model development	Cross section processing and deterministic methods completion	Develop/examine 2-D SCALE “slab” model Documentation/archive VENTURE models Transport methods (ATTILA[19])
	MCNP model development	Develop discrete plate representation model Revise geometry to generate smaller volume zones in fuel region Update/make operational MCNP depletion model (MONTEBURNS[20]) Research publications for LEU validation; develop plan for LEU validation studies
	Turbulent mixing, non-bond assumptions in thermal-hydraulic model	Incorporate into HFIR steady state heat transfer code; validate
	Probabilistic combination of uncertainties	Review/update TASHA code developed under Advanced Neutron Source Program
Program management	Activities	Report preparation Travel Review committees

increased from about 70 MW to 85 MW or even above 85 MW. An examination will be conducted of the use of axial neutron poison zones and poisoned sideplates as a means of improving HFIR power distribution, by reducing the power peaking.

The use of a 1-D grading results in power peaking near the upper and lower edges of the fuel plates because these regions are near the light-water coolant. To increase the thermal margins and increase or regain the HFIR full operating power, it is necessary to reduce the power peaking in these regions. The use and assessments of a 2-D grading will result in an optimal power distribution and will greatly reduce this power peaking. A 2-D fuel grading was developed for the Advanced Neutron Source (ANS) reactor,* and a similar methodology will be applied to the HFIR design. A 2-D, continuously graded, monolithic U-10Mo fueled HFIR case, with a 127-μm (5-mil) limit on the fuel-meat thickness, will be developed. Neutron flux, power density, reactor physics and safety parameters, and core lifetime and reactivity behavior will be assessed.

Studies reported in this document have shown that a primary performance indicator – neutron flux at the cold source location—is reduced by 15% with LEU fuel in HFIR at 85 MW. Increasing the HFIR power level to the original design value of 100 MW would eliminate this penalty. If 1-D or 2-D graded designs can be found that allow for an operating power greater than 85 MW, an engineering/economic assessment will be conducted of the cost and schedule required to return HFIR operating power to 100 MW.

MCNP model development will be conducted to support transition from deterministic reactor physics models to Monte Carlo models as the basis for design and safety analyses. A necessary step in the transition to Monte Carlo methods is the verification and validation (V&V) process. The first step is to identify available and relevant benchmark data for the methods. This will include the calculation of relevant high-flux LEU experiments or benchmark cases. Where possible, benchmark comparisons will be made against intermediate spectrum reactor benchmark cases in the International Criticality Safety Benchmark Evaluation Project (ICSBEP) database. One possible relevant case is the 30-MW Oak Ridge Research (ORR) reactor in its final cycle. For this cycle, data exist for HEU oxide and LEU silicide fuel, including burnup data.

Two methods-development tasks are proposed, both of which should increase the operating power for the reactor. These include revision of the thermal-hydraulic code to include more accurate models of coolant flow and heat transfer through and around “non-bonds” of the fuel to the clad. A second task involves the use of statistical thermal-hydraulic uncertainty analysis to assess the effects of the HFIR HEU-to-LEU fuel conversion.

Typically, reactor acceptance criteria are established by thermal-hydraulic parameters (critical heat flux, peak temperatures, flow excursion limit, etc.), and thermal-hydraulic analyses are used to establish the operation margins. In order to meet regulatory requirements, parameter uncertainties must be accounted for in these analyses. Early analyses relied on conservative treatment of these uncertainties; however, this approach “stacked” uncertainties, and possibly provided overly conservative limits. The use of statistical uncertainty treatment decreases conservatism and also provides a method to quantify the uncertainty level of the calculational results.

The work proposed here will use statistical uncertainty analysis to evaluate the thermal-hydraulic impact of using LEU fuel in HFIR. This effort will be based on existing work that was performed in support of the ANS reactor project, where statistical uncertainty analysis was used to perform steady state thermal-hydraulic analysis of a reactor of similar geometry and manufacture as HFIR. In the ANS project, the code package SAMPLE (a statistical analysis code) was combined with a steady state thermal-hydraulic analysis code for involute fuel plate core designs, TASHA, to perform statistical thermal-hydraulic uncertainty analysis that examined thermal-hydraulic limits in the core (flow

*J. C. Gehin, J. P. Renier, and B. A. Worley, “A New Fuel Loading Design for the Advanced Neutron Source,” *Proc. Top. Meet. on Reactor Physics, April 11–15, 1994, Knoxville, Tennessee*, American Nuclear Society (April 1994).

excursion, incipient boiling, etc.). This code package will be installed on existing computing platforms and evaluated for differences between ANS design, the HFIR HEU design, and the HFIR/LEU design. Sample cases will be run using preliminary core specifications and a preliminary set of uncertainties for a LEU core design. Three types of sample analyses will be exercised: one using a traditional conservative uncertainty approach, one using a statistical peaking factor based approach, and one using direct input of uncertainty distributions to the thermal-hydraulic analysis package. This task will prepare the codes to accept future code modifications as the LEU concept matures and to perform thermal-hydraulic analysis that will help guide the core design effort.

Funding is requested to support the preparation of presentations and reports on the activities of the core conversion. This task also includes support for a review committee, meeting attendance, and associated travel.

ORNL has proposed to provide support to the fuel development program of the RERTR. Fuel development activities are itemized in Table 6.2. The activities are in two categories—support to irradiations being conducted by the RERTR program in the Advanced Test Reactor (ATR) (diffractometry measurements) and review and advice on fuel development. Review of ATR results is included in the program management task; advice on development of a 2-D fabrication procedure is included in the "Graded fuel development program" task. The graded fuel development program supports the comment from the HFIR Executive Director that "we do believe that a technology breakthrough will be required" yet seeks to achieve this development in a structured and logical fashion with as much cooperation among interested parties as can be achieved.

Table 6.2. Fuels development activities proposed for FY 2007

Task name		Start date or comment
Graded fuel development program		Collaboration with FRM reactor staff and FRM fuel fabricator (CRCA/ARIVA) on physical vapor deposition processes for fabricating 2-D grading and monolith diffusion barrier
Diffractometry measurements—as requested by RERTR program (Next HFIR cycle expected December 2006; HFIR staff recommend RERTR plan for cycle after startup; March 2007)	Sample preparation and transportation inside ORNL	3 months prior to HFIR startup
	Measurement preparation, measurement, post-measurement analyses	2 months prior to HFIR startup
	Planning for measurements to support revision of safety basis documents	November 2006
Fuels program management		Includes support to review committees, meeting attendance, travel, and report preparation

7. REFERENCES

1. R. T. Primm III, R. J. Ellis, J. C. Gehin, D. L. Moses, J. L. Binder, and N. Xoubi, *Assumptions and Criteria for Performing a Feasibility Study of the Conversion of the High Flux Isotope Reactor Core to Use Low-Enriched Uranium Fuel*, ORNL/TM-2005/269, February 2006.

2. N. Xoubi and R. T. Primm III, *Modeling of the High Flux Isotope Reactor Cycle 400*, ORNL/TM-2004/251, Oak Ridge National Laboratory, Oak Ridge, Tennessee, August 2005.

3. D. E. Peplow, *A Computational Model of the High Flux Isotope Reactor for the Calculation of Cold Source, Beam Tube, and Guide Hall Nuclear Parameters*, ORNL/TM-2004/237, Oak Ridge National Laboratory, Oak Ridge, Tennessee, November 2004.

4. N. Xoubi, R. T. Primm III, and G. I. Maldonado, "A Computational Model of the High Flux Isotope Reactor—Validation and Application to Low Enriched Uranium Fuels," *Proceedings of the Joint Conference, International Group on Research Reactors and Test, Research, and Training Reactors*, 2005.

5. C. O. Slater and R. T. Primm III, *Calculation of Rabbit and Simulator Worth in the HFIR Hydraulic Tube and Comparison with Measured Values*, ORNL/TM-2005/94, Oak Ridge National Laboratory, Oak Ridge, Tennessee, September 2005.

6. N. Xoubi and R. T. Primm III, *Investigation of Beryllium Internal Reflector Installation on the Fuel Cycle Length of the High Flux Isotope Reactor*, ORNL/TM-2004/252, August 2005.

7. R. T. Primm III, R. J. Ellis, and J. C. Gehin, *Preliminary Report, Design Study for a Low Enriched Uranium (LEU) Core for the High Flux Isotope Reactor (HFIR)*, ORNL/TM-2006/80, April 20, 2006

8. R. T. Primm III, R. J. Ellis, J. C. Gehin, D. L. Moses, J. L. Binder, and N. Xoubi, "Assumptions and Criteria for Performing a Feasibility Study of the Conversion of the High Flux Isotope Reactor Core to Use Low-Enriched Uranium Fuel," *Paper 157386, Proceedings of the American Nuclear Society PHYSOR-2006 International Topical Meeting on Reactor Physics: Advances in Nuclear Analysis and Simulation, Vancouver, Canada, September 2006.*

9. R. J. Ellis, J. C. Gehin, and R. T. Primm III, "Cross Section Generation and Physics Modeling in a Feasibility Study of the Conversion of the High Flux Isotope Reactor Core to Use Low-Enriched Uranium Fuel," *Paper 157797, Proceedings of the American Nuclear Society PHYSOR-2006 International Topical Meeting on Reactor Physics: Advances in Nuclear Analysis and Simulation, Vancouver, Canada, September 2006*.

10. *HFIR Updated Safety Analysis Report*, ORNL/HFIR/USAR/2344, Rev. 5, Oak Ridge National Laboratory, Oak Ridge, Tennessee, May 2005.

11. R. D. Cheverton and T. M. Sims, *HFIR Core Nuclear Design*, ORNL-4621, Oak Ridge National Laboratory, Oak Ridge, Tennessee, 1971.

12. R. T. Primm III, *Reactor Physics Input to the Safety Analysis Report for the High Flux Isotope Reactor*, ORNL/TM-11956, Oak Ridge National Laboratory, Oak Ridge, Tennessee, March 1992.

13. D. R. Vondy, T. B. Fowler, and G. W. Cunningham III, *The Bold Venture Computation System for Nuclear Reactor Core Analysis, Version III*, ORNL-5711, Oak Ridge National Laboratory, Oak Ridge, Tennessee, June 1981.

14. N. Xoubi, *Characterization of Exposure-Dependent Eigenvalue Drift Using Monte Carlo Based Nuclear Fuel Management*, Ph.D. Dissertation, University of Cincinnati, November 2005.

15. *SCALE: A Modular Code System for Performing Standardized Computer Analyses for Licensing Evaluations*, ORNL/TM-2005/39, Version 5, Vols. I–III, Oak Ridge National Laboratory, Oak Ridge, Tennessee, April 2005. [Available from Radiation Safety Information Computational Center (RSICC) at Oak Ridge National Laboratory as CCC-725.]

16. *MCNP—A General Monte Carlo N-Particle Transport Code, Version 5*, LA-CP-03-0245, Los Alamos National Laboratory, April 2003.

17. R. T. Primm III, *Reactor Physics Studies of Reduced-Tantalum-Content Control and Safety Elements for the High Flux Isotope Reactor*, ORNL/TM-2003/65, December 2003.

18. H. A. McLain, *HFIR Fuel Element Steady State Heat Transfer Analysis*, Revised Version, ORNL/TM-1904, Oak Ridge National Laboratory, Oak Ridge, Tennessee, December 1967 as appended by T. E. Cole, L. F. Parsly, and W. E. Thomas, *Revisions to the HFIR Steady State Heat Transfer Analysis Code*, ORNL/CF-85/68, April 7, 1986.

19. ATTILA computer code Web page: http://www.radiative.com/software.htm.

20. D. L. Poston and H. R. Trellue, *User's Manual, Version 2.0 for MONTEBURNS Version 1.0*, Los Alamos National Laboratory, LA-UR-99-4999 (September 1999).

Appendix A. COMMENTARY ON CALCULATED POWER DISTRIBUTIONS FOR HFIR

Computational methods based on the neutron diffusion theory, the VENTURE code for HFIR (Refs. 1, 13), were used to predict parameters, both for HEU and LEU cycles, such as HFIR cycle life time, critical mass, peak thermal neutron flux levels in the beryllium reflector, peak thermal neutron flux levels in the central flux trap target region, and isotopic concentrations as a function of fuel burnup. For the current HEU cycle, calculated values are frequently within a few percent of measured values (Ref. 12). Likewise, comparison to measured values shows that local power density estimates can be accurately calculated at many locations in the reactor core. However, the power distribution at the edges of the fuel plates in the inner fuel element and the outer fuel element as predicted with diffusion theory are not as accurate as the previously mentioned integral parameters and tend to be significantly greater than the measured values. This is due to regions of high fissile content (strong absorbers) being adjacent to relatively weak absorbers (a water-filled region or a beryllium region); diffusion theory being known to be inaccurate in such conditions. Consequently, the current safety analysis (Refs. 10, 11) for the HEU core in HFIR is based on neutron diffusion theory corrected by experimental results. These measurements were made in 1965 and 1966 as a part of the startup tests for HFIR.

There were no experiments that could be used to correct the neutron diffusion theory LEU core calculations in the manner that was done for the HEU core. To address the lack of pertinent LEU experimental results for HFIR, Monte Carlo neutron transport theory methods (MCNP) were used to calculate fuel plate local power densities and regional power generation information. These Monte Carlo results were used in the heat transport and thermal safety assessments to determine the maximum HFIR operational power. The use of power densities from MCNP was appropriate because the highest local power densities occur at beginning-of-cycle (BOC).

The use of Monte Carlo methods with fuel depletion could, similarly, improve the accuracy of the LEU HFIR power distribution at time intervals following BOC. These methods have been investigated (Ref. 14), but found to be too limiting and cumbersome for fuel element design as well as being unnecessary because the limiting condition for operation occurs at BOC.

It is noteworthy that using MCNP-derived power densities for the current HEU core as input to the HFIR steady-state heat transfer program yields an allowable operating power of 91.07 MW. The same program executed with experiment-corrected diffusion theory—the power distribution that is the current basis for the HFIR Safety Analysis Report—yields 85.1 MW (the current maximum operating power for the HFIR is 85 MW). Diffusion theory-derived power densities uncorrected with experimental measurements yield an operating power of 72 MW.

The calculations reported in this document are based on MCNP-derived power profiles. It is an unresolved question as to whether the HEU results indicate that the MCNP calculations are biased high (and so indicating that a factor of 85.1/91.07 = 0.934 should be applied to operating powers determined using input from MCNP calculations). The authors of this work believe that the experimental uncertainties in the power distributions that are reported in Ref. 11 are such that a bias factor cannot be justified and so has not been applied. The authors also believe that these results demonstrate that power distribution measurements would be required prior to full-power operation with LEU. As indicated in Section 4, these required tests will impact the cost of conversion.

Appendix B. CROSS SECTION PROCESSING AND METHOD FOR ESTABLISHING CYCLE LENGTH

The nuclear data libraries used with the neutronics codes were based on ENDF/B-V and VI nuclear data. The libraries used with BOLD VENTURE (Ref. 13) are ISOTXS libraries prepared using SCALE cross-section generation and the SCALE 238-group ENDF/B-V master libraries (Ref. 15). The few-group cross section library for the BOLD VENTURE analysis is created using modules for resonance processing followed by a one-dimensional radial calculation using SCALE sequences to obtain the appropriate neutron flux spectrum for collapsing the cross sections to 20 neutron energy groups (sequence includes (BONAMI, NITAWL, and XSDRNPM modules). Table B.1 shows the neutron energy structure of the 20-group set of collapsed energy groups with a comparison to the groups of the 238 neutron-energy group nuclear data master library. In the past, the ISOTXS library that was produced by the SCALE/AMPX script contained seven energy groups and the combination of older and current calculations led to some incorrect flux ratios being reported in Ref. 7.

The cross section data for this work was prepared using a SCALE/AMPX LINUX script that originated from a revision to work documented in Ref. 12. For the work presented in this report, the LINUX scripts were adapted to use the ENDF/B-V SCALE 238 neutron energy group master library (Ref. 15). In addition, four, new, lumped fission product representations were created and used in the HFIR LEU work.

The geometry and spatial regions used in the VENTURE cases are exactly represented in the LEU cross section preparation script in the SCALE/XSDRN input. Several regionally specific "isotopes" have been set up for ^{235}U and ^{238}U to better represent the reaction rates at the inner edge of the IFE fuel plates.

Table B.1. Structure of the collapsed neutron energy group

Energy group number for 20-group library	Lowest-energy group number for 238-group library that is included in the collapsed structure	Lower energy limit (eV)
1	12	$2.479 \times 10^{+06}$
2	15	$1.50 \times 10^{+06}$
3	25	$8.75 \times 10^{+05}$
4	45	$8.50 \times 10^{+04}$
5	63	$2.58 \times 10^{+03}$
6	86	$9.00 \times 10^{+01}$
7	116	$2.75 \times 10^{+01}$
8	132	$9.10 \times 10^{+00}$
9	149	$2.97 \times 10^{+00}$
10	163	$1.68 \times 10^{+00}$
11	190	9.75×10^{-01}
12	199	6.25×10^{-01}
13	205	3.75×10^{-01}
14	210	2.50×10^{-01}
15	215	1.25×10^{-01}
16	222	4.00×10^{-02}
17	226	7.50×10^{-03}
18	230	2.50×10^{-03}
19	232	1.50×10^{-03}
20	238	1.00×10^{-05}

The script for use with the HEU case was prepared with a minimum of changes to the existing QA-documented SCALE/AMPX input (Ref. 12). The major difference is the use of the 238-group master library and the new lumped fission product data.

The results from VENTURE calculations for the k_{eff} behavior of the LEU core fuel designs compared to the reference HEU case are presented in Fig. B.1. The cases are without control absorber insertion to illustrate the excess reactivity behavior of the various cores. Both the HEU and LEU cores in HFIR show the expected significant drop in available core reactivity during the first day of operation due to the build-in of the fission product poison ^{135}Xe. The larger drop for LEU relative to HEU is due to the impact on reactivity of neutron energy spectral differences as fission products build-in (see Figs. 2.5 and 2.6). The reactivity of the LEU cores at 26 d is seen to be similar to the reference HEU core case. This implies that while the uranium mass to meet core lifetime is approximately correct, some small revision could be expected to exactly match cycle lengths for the two cycles. The authors think that the revision would be insignificantly small.

In Fig. B.2, the k_{eff} vs full-power days of operation are shown for the no-minimum-thickness LEU and HEU cases with control absorber movement simulated. While cycle length can be estimated from the cases shown in Fig. B.1, the "correct" power distribution as a function of time must be obtained from the cases illustrated in Fig. B.2 to correctly estimate as a function of operating time the peak local power density, peak local burnup, maximum clad oxide thickness, and any other "local" parameters of interest that are time and position dependent.

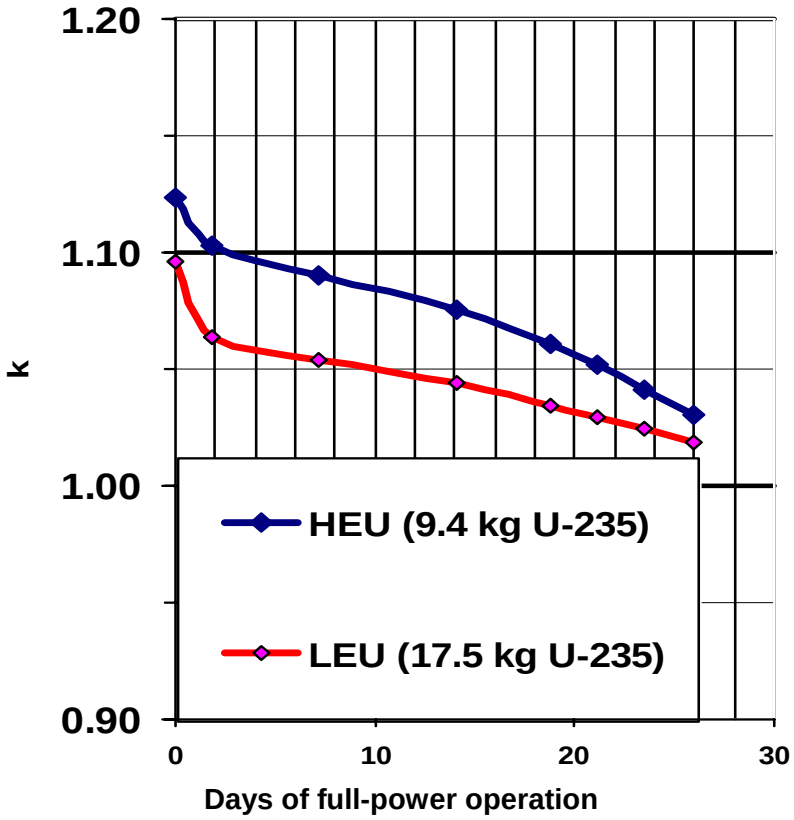

Fig. B.1. Comparison of k vs time for the LEU and HEU cores (without control absorber insertion) as calculated with VENTURE.

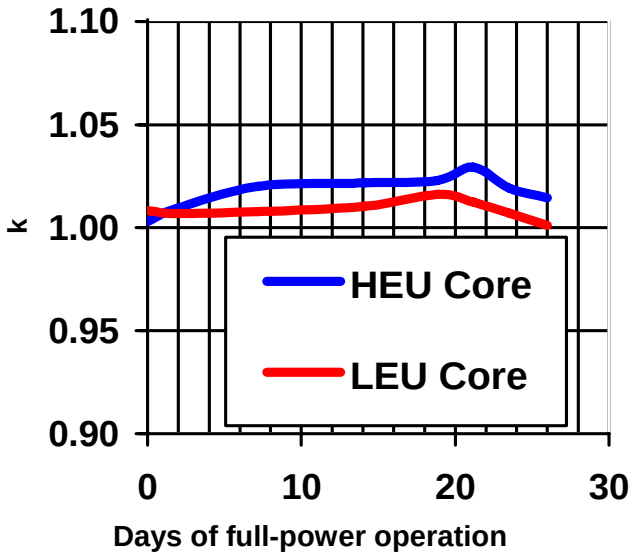

Fig. B.2. Simulated operating criticality by modeled control absorber movement.

Figure B.3 compares the behavior of the uncontrolled k-effective as a function of full-power (85-MW) days of HFIR operation for the reference HEU core and the LEU core with no minimum thickness. The HEU core has a larger reactivity at BOL and drops, generally, at a greater rate than the LEU case. The LEU core generates more fissile plutonium during its lifetime than the HEU core, and this offsets the utilization of the ^{235}U during the life cycle. The two curves meet just after 26 d of reactor operation.

As seen in Fig. B.3, the reactivity of the various HFIR cores depends on the composition and design of the fueling options. The HEU core has the most reactivity at BOL, but k_{eff} drops quickly in the simulations. The LEU cases have initial reactivity that is dependent on the amount of ^{235}U in the core.

The "LEU" case is the monolithic no-minimum-thickness design, with optimized grading. The grading optimization involved iterative physics/thermal-hydraulics calculations to minimize the enthalpy increases in the hottest streaks.

The coated and uncoated dispersion cases denoted as "cases 1" have a grading shape proportional to the LEU no-minimum-thickness case, and the limit for the fuel is such that the fuel meat thickness cannot exceed 27.1 mils at the thickest point. The "case 2" options for coated and uncoated LEU dispersion fuel are the other extreme: as much fuel material as possible is modeled into the fuel plates, again with a maximum thickness of 27.1 mils, but for a large portion of the fuel plates. The intent was to get as close to 17.5 kg of ^{235}U as possible. The power density and enthalpy increases are definitely not optimized for these "case 2" options, and invariably, as currently designed, these cores would have to operate at a reduced HFIR power. The "case 1" options can operate close to 85 MW, but the reduced available reactivity limits the core lifetime, as is evident in the k_{eff} vs time curves.

In summary, from the information presented in Fig. B.3, the cycle length for the HEU case, as defined by a chosen target end-of-life k_{eff} of 1.015, would be 29 d of full-power operation. The difference between the actual cycle length of 26 days and the uncontrolled calculated value is due to the choice of the target k_{eff} and also the light irradiation loading of the reference case compared to actual cycles. Also, there will be effects caused by changes in power distribution (and therefore local burnup and local nuclide concentrations) in the uncontrolled case due to the absence of the control elements. Nevertheless, these uncontrolled cases are useful for predicting relative changes in lifetime due to changes in fuels. The unconstrained thickness LEU monolithic case has a calculated lifetime of

28 d. The uncoated dispersion fuel (case 1) has a calculated lifetime of 22 d. The coated dispersion fuel (case 1) has a calculated lifetime of 11 d. The uncoated dispersion fuel (case 2) has a calculated lifetime of 32 d. The coated dispersion fuel (case 2) has a calculated lifetime of 36 d. These values were used to determine the expected end-of-cycle burnup values that are reported in Table 3.1. More accurate estimates can be obtained by determining critical control element position for selected times for each fuel cycle, and these can be performed in FY 2007.

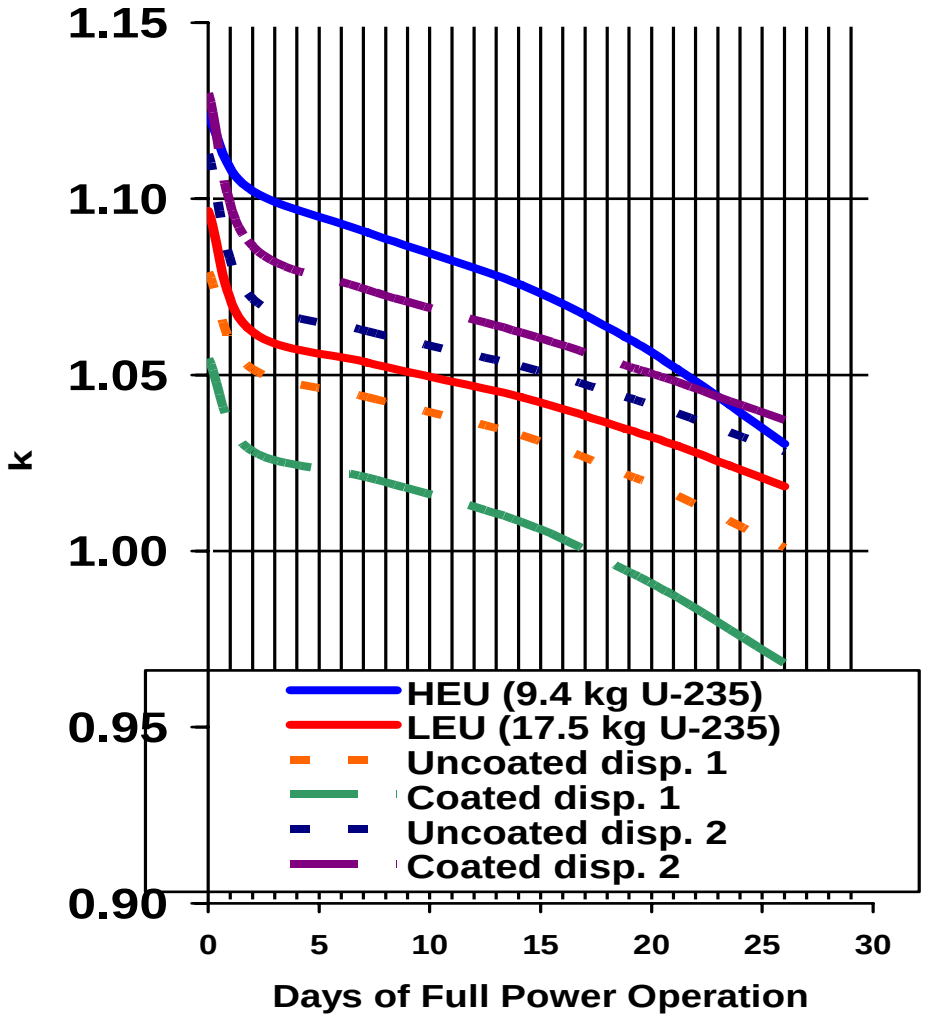

Fig. B.3. Simulated uncontrolled k_{eff} vs full-power days of operation.

Appendix C. METHODOLOGY FOR SAFETY-RELATED COEFFICIENTS OF REACTIVITY

The Doppler effect was calculated for the various cases by preparing ISOTXS libraries at the two reference fuel temperatures (300 K and 500 K) in the SCALE/AMPX modules (BONAMI, NITAWL, and XSDRN). The Doppler data presented in the Table 2.5 are the total k1-k2/k1k2 reactivity difference from the corresponding time step k values from the VENTURE output, for cases with the appropriate ISOTXS libraries. In addition to the total reactivity differences, the Doppler coefficient in terms of degrees K © and degrees F are also shown. It is evident that the Doppler effect is about ten times larger for the LEU case than the HEU case, which is expected in consideration of the large concentration of ^{238}U in the LEU case.

The void coefficients were calculated by changing the H and O atom densities in the VENTURE case material definitions by 10% (reduction) to represent a 10% void. The calculations were performed in either IFE or OFE regions (only). The calculations of the void reactivity coefficient for the HEU IFE and OFE, at BOL, are close to the experimental HFIR results of –0.080 and –0.170, respectively. The LEU and HEU cores have similar core void reactivity coefficients.

Similarly, the void reactivity effect for the target region (FTT) is also modeled for a 10% reduction in the LW coolant density. The void effects are seen to be positive for both the LEU and HEU cases, as expected, and the magnitude of the LEU case values is slightly smaller than the HEU case values.

Appendix D. INPUT FOR DECAY-HEAT AND GAMMA DOSE RATE CALCULATIONS

The methodology for calculating the gamma dose rates for the HFIR core, and the IFE and OFE individually, is documented in C-HFIR-2005-146 (available from the Director of the Research Reactors Division, Oak Ridge National Laboratory). This documented methodology included the use of SCALE 4.3 and 4.4 (ORIGEN and SAS1). For the current work, SCALE5 was used (which includes various improvements in these SCALE modules). SCALE5/ORIGEN allows the user to input the precise gamma energy spectrum desired for the gamma source calculations. The gamma energy information was input so that the ORIGEN output in 18 groups could be used directly with SAS1 in an XSDOSE calculation. The ORIGEN case output parameters were modified to allow for the output of decay heat information for actinides and fission products at various cooling times.

The decay heat, gamma source, and dose rate calculations were performed for both the reference HEU case, and the no-minimum-thickness LEU case. The ORIGEN input data were chosen to yield exactly 26 d of operation (2210 MWd) at precisely 85 MW for both the HEU and the LEU core cases.

The ORIGEN-S calculations determine the contributions to fission product decay heat from more than 1100 nuclides, as summarized in Table D.1. About 800 nuclides give nonnegligible α, β, and γ decay heat contributions to the discharged LEU and HEU HFIR core decay heats.

Table D.1. Decay heat (W) for the HFIR HEU and LEU cores

Decay heat		Discharge	1 year	5 years	30 years
HEU	Actinides	$4.099 \times 10^{+3}$	3.861×10^{-1}	3.823×10^{-1}	3.472×10^{-1}
	FP	$4.409 \times 10^{+6}$	$1.409 \times 10^{+3}$	$1.123 \times 10^{+2}$	$4.182 \times 10^{+1}$
	Total	$4.413 \times 10^{+6}$	$1.409 \times 10^{+3}$	$1.127 \times 10^{+2}$	$4.217 \times 10^{+1}$
LEU	Actinides	$7.854 \times 10^{+4}$	$1.234 \times 10^{+0}$	$1.245 \times 10^{+0}$	$1.262 \times 10^{+0}$
	FP	$5.024 \times 10^{+6}$	$1.401 \times 10^{+3}$	$1.094 \times 10^{+2}$	$4.124 \times 10^{+1}$
	Total	$5.103 \times 10^{+6}$	$1.402 \times 10^{+3}$	$1.106 \times 10^{+2}$	$4.250 \times 10^{+1}$

Overall, the LEU HFIR core fission product decay heat source at discharge (t = 0) is about 14% greater than the HEU HFIR core decay heat source. The largest FP decay heat contributor at discharge is ^{134}I for both the LEU and HEU cores, with the LEU contribution being about 1.14 times greater, 101.7 kW vs 89.1 kW. The overall difference in decay heat for the LEU and HEU discharged cores is the result of the fission product composition of the fuel. Table D.2 shows the fission power in the HFIR cores at EOL resulting from fissions in the main fissionable nuclides. The table also presents the total number of fissions that occurred in these nuclides over the 2210-MWd (26-d) HFIR fuel cycle simulation calculations. The fission product yields vary from nuclide to nuclide and also depend on the incident neutron energies.

Table D.2. Power (at EOL) and total fissions during the LEU and HEU HFIR core fuel cycles

Nuclide	LEU		HEU	
	Power (W)	Fissions	Power (W)	Fissions
^{239}Pu	$3.929 \times 10^{+6}$	$1.197 \times 10^{+17}$	$3.507 \times 10^{+5}$	$1.068 \times 10^{+16}$
^{241}Pu	$1.120 \times 10^{+5}$	$3.388 \times 10^{+15}$	$2.584 \times 10^{+4}$	$7.817 \times 10^{+14}$
^{235}U	$7.803 \times 10^{+7}$	$2.479 \times 10^{+18}$	$8.338 \times 10^{+7}$	$2.649 \times 10^{+18}$
^{238}U	$1.445 \times 10^{+6}$	$4.308 \times 10^{+16}$	$1.109 \times 10^{+4}$	$3.507 \times 10^{+14}$

As cooling time increases, the fission product decay heat from LEU and HEU HFIR cores become similar. Table D.3 shows the top contributors after 1 year of cooling; the decay heat from the HEU core is slightly greater than for the LEU core.

Table D.3. Comparison of LEU and HEU FP decay heat contributions after 1 year of cooling

Nuclide	Decay heat (W)	
	LEU	**HEU**
^{144}Pr	733	742
^{95}Nb	224	226
^{95}Zr	111	111
^{106}Rh	85.1	68.2
^{144}Ce	65.3	66.1
^{91}Y	53.4	54.1
^{90}Y	38.9	39.9
^{137m}Ba	26.8	27.0
^{89}Sr	23.2	23.6
^{147}Pm	8.41	7.65
^{90}Sr	8.16	8.36
^{137}Cs	8.04	8.08
^{103}Ru	4.44	4.20
^{134}Cs	4.33	16.6
^{85}Kr	1.35	1.39
^{154}Eu	1.32	0.772
^{125}Sb	1.14	1.10
^{141}Ce	1.08	1.07
^{106}Ru	0.528	0.423
^{144m}Pr	0.480	0.486
Total	*1400*	*1408*

Appendix E. CALCULATION OF TEMPERATURE PROFILE INSIDE A FUEL PLATE

From Fig. 2.4, the highest local power density occurs at the axial midplane of the outer element, at the outside edge of the element. From Table 2.2, the thickness of the U-10Mo region at this location is 170 μm. Heat flux, oxide thickness, and clad surface temperature as a function of time were computed using the HFIR steady state heat transfer program. The HEATING program was used to compute the nominal operating temperature distribution inside the fuel plate at this spot.

The HEATING computer program is a part of the SCALE system. HEATING is a general purpose, conduction heat transfer program and can solve steady-state and/or transient heat conduction problems in one-, two-, or three-dimensional Cartesian, cylindrical, or spherical coordinates.

A one-dimensional model of a HFIR fuel plate was created. The boundary condition at the fuel plate clad surface was assumed to be 117°C (240.3°F) based on the results of the HFIR steady state heat transfer program. The U-10Mo was assumed to be coated with 25.4 μm (1-mil) thick niobium. Material properties (densities, thermal conductivites, etc.) were taken from the SCALE material property library that is a part of, and distributed with, the SCALE system. The calculated maximum temperature in the U-10Mo region is 137°C (278°F). The heat flux at this location is 322 W/cm^2 and the local-to-core-average power density ratio is 1.51.

Because of coolant downflow, the buildup of oxide on the fuel plate, and the radially dependent, axially averaged power distribution, the peak clad temperature does not occur at the neutronic hot spot but rather occurs in the inner element plate at 2.40 cm along the plate and at the bottom edge of the fuelled zone of the plate. The fuel thickness at this point is 165 μm. The maximum temperature in the U-10Mo region at the location of the highest clad temperature is 144°C (291°F). The heat flux at this location is 235 W/cm^2, and the local-to-core-average power density ratio is 1.101.

As noted in the body of the report, the operating power for the HFIR is determined by applying margins-of-safety to the predicted incipient boiling conditions. At just below the incipient boiling conditions, the peak clad temperature would be 212°C (413°F). The incipient boiling heat flux at this location would be 304 W/cm^2. Note that the maximum local heat flux in the core at incipient boiling conditions would be 417 W/cm^2.

All values for heat flux and temperatures reported in this appendix are for beginning-of-life (BOL) conditions. Because the neutronic peak power density at BOL occurs at the core-Be interface and since the maximum clad temperature value occurs at the lower edge of the fuel zone (fuel-water interface), it is questionable that diffusion theory calculations, unadjusted with experiments, can be used to predict temperatures at these locations as a function of time. Depletion Monte Carlo calculations are needed but are beyond the scope of the current fiscal year's effort.

INTERNAL DISTRIBUTION

1. S. T. Baker (bakerst@ornl.gov)
2. K. J. Beierschmitt (beierschmitt@ornl.gov)
3. J. L. Binder (binderjl@ornl.gov)
4. E. E. Bloom (bloomee@bellsouth.net)
5. C.A. Blue (blueca@ornl.gov)
6. S. E. Burnette (burnettese@ornl.gov)
7. C. W. Coates (coatescw@ornl.gov)
8. B. S. Cowell (cowellbs@ornl.gov)
9. D. C. Christensen (christensend@ornl.gov)
10. R. A. Crone (cronera@ornl.gov)
11. R. J. Ellis (ellisrj@ornl.gov)
12. J. C. Gehin (gehinjc@ornl.gov)
13. T. J. Huxford (huxfordtj@ornl.gov)
14. G. M. Ludtka (ludtkagm1@ornl.gov)
15. S. B. Ludwig (ludwigsb@ornl.gov)
16. C. R. Luttrell (luttrellcr@ornl.gov)
17. I. Moldonado (Ivan.Maldonado@uc.edu)
18. D. L. Moses (mosesdl@ornl.gov)
19. S. D. Moses (mosessd@ornl.gov)
20. L. Ott (ottlj@ornl.gov)
21. C. V. Parks (parkscv@ornl.gov)
22. M. A. Pershing (pershingma@ornl.gov)
23. L. P. Phillips (phillipslpjr@ornl.gov)

24–26. R. T. Primm III (primmrtiii@ornl.gov)

27. L. D. Proctor (proctorld@ornl.gov)
28. R. R. Rawl (rawlrr@ornl.gov)
29. A. W. Riedy (riedyaw@ornl.gov)
30. J. E. Rushton (rushtonje@ornl.gov)
31. L. J. Satkowiak (satkowiaklj@ornl.gov)
32. J. D. Sease (seasejd@ornl.gov)
33. K. A. Smith (smithka@ornl.gov)
34. R. L. Snipes (snipesrl@ornl.gov)
35. C. C. Southmayd (southmaydcc@ornl.gov)
36. M. R. Uzzle (uzzlemr@ornl.gov)
37. J. M. Vitek (vitekjm@ornl.gov)
38. J. M. Whitaker (whitakerjm@ornl.gov)
39. S. J. Zinkle (zinklesj@ornl.gov)
40. ORNL Laboratory Records (hamrindr@ornl.gov)

EXTERNAL DISTRIBUTION

41. T. Andes, BWXT/Y-12, Y-12 National Security Complex, P.O. Box 2009, Oak Ridge, TN 37831-8245 (andestc@y12.doe.gov)
42. R. A. Butler, Director, Research Reactor Center, 1513 Research Park Drive, Columbia, MO 65211 (ButlerRa@missouri.edu)
43. G. S. Chang, Idaho National Laboratory, P.O. Box 1625, Idaho Falls, ID 83415-3885 (gray.chang@inl.gov)
44. D. Chong, NA-212, United States Department of Energy, Washington, D.C. (Daniel.Chong@nnse.doe.gov)
45. H. E. Clark, United States Department of Energy Oak Ridge Office, P.O. Box 2001, Oak Ridge, TN 37831 (hkc@ornl.gov)
46. G. Copeland, c/o David Moses, P.O. Box 2008, Oak Ridge, TN 37831-6050 (copelandgl@ornl.gov)
47. H. D. Gougar, Manager, Fission & Fusion Systems, INEEL, P.O. Box 1625, MS 3860, Idaho Falls, ID 83415-3860 (goughd@inl.gov)
48. M. Hassler, BWXT/Y-12, Y-12 National Security Complex, P.O. Box 2009, Oak Ridge, TN 37831-8245 (hasslerme@y12.doe.gov)
49. M. Hutmaker, U.S. Department of Energy, 1000 Independence Ave. SW, Washington, DC 20585 (matthew.hutmaker@nuclear.energy.gov)
50. D. Kutikkad, Assistant Reactor Manager-Physics, University of Missouri Research Reactor Facility, Columbia, MO 65211 (kutikkadk@missouri.edu)

51. J. Matos, Argonne National Laboratory, 9700 S. Cass Avenue, Argonne, IL 60439 (jim.matos@anl.gov)
52. C. McKibben, University of Missouri Research Reactor Facility, Columbia, MO 65211 (mckibben@missouri.edu)
53. D. M. Meyer, Idaho National Laboratory, P.O. Box 1625, Idaho Falls, ID 83415-3750 (Dana.Meyer@inl.gov)
54. M. K. Meyer**,** Idaho National Laboratory, P.O. Box 1625, Idaho Falls, ID 83415-6188 (Mitchell.Meyer@inl.gov)
55. T. Newton, MIT Nuclear Reactor Laboratory, 138 Albany St., Cambridge, MA 02139 (tnewton@mit.edu)
56. B. Nielson, Idaho National Laboratory, P.O. Box 1625, Idaho Falls, ID 83415-3890 (Bruce.Nielson@inl.gov)
57. W. Richards, NIST Center for Neutron Research, 100 Bureau Drive, Stop 8561, Gaithersburg, MD 20899-8561 (wade.richards@nist.gov)
58. J. Roglans, Argonne National Laboratory, 9700 S. Cass Avenue, Argonne, IL 60439 (roglans@anl.gov)
59. J. Snelgrove, Argonne National Laboratory, 9700 S. Cass Avenue, Argonne, IL 60439 (jimsnelgrove@anl.gov)
60. P. Staples, NA-212, United States Department of Energy, Washington, D.C. (Parrish.Staples@nnsa.doe.gov)
61. R. E. Williams, NIST Center for Neutron Research, 100 Bureau Drive, Stop 8560, Gaithersburg, MD 20899-8560 (robert.williams@nist.gov)